Quaternary Science Reviews 148 (2016) 128–145

Contents lists available at ScienceDirect

Quaternary Science Reviews

journal homepage: www.elsevier.com/locate/quascirev

Distribution and characteristics of overdeepenings beneath the Greenland and Antarctic ice sheets: Implications for overdeepening origin and evolution

H. Patton [a, b, 1], D.A. Swift [a, *], C.D. Clark [a], S.J. Livingstone [a], S.J. Cook [c]

[a] Department of Geography, University of Sheffield, Winter Street, Sheffield, S10 2TN, UK
[b] CAGE—Centre for Arctic Gas Hydrate Environment and Climate, Department of Geology, UiT The Arctic University of Norway, 9037, Tromsø, Norway
[c] School of Science and the Environment, Manchester Metropolitan University, Chester Street, Manchester, M1 5GD, UK

ARTICLE INFO

Article history:
Received 5 February 2016
Received in revised form
8 July 2016
Accepted 11 July 2016
Available online 21 July 2016

Keywords:
Glacial erosion
Landscape evolution
Overdeepening
Geomorphology
Ice sheet

ABSTRACT

Glacier bed overdeepenings are ubiquitous in glacier systems and likely exert significant influence on ice dynamics, subglacial hydrology, and ice stability. Understanding of overdeepening formation and evolution has been hampered by an absence of quantitative empirical studies of their distribution and morphology, with process insights having been drawn largely from theoretical or numerical studies. To address this shortcoming, we first map the distribution of potential overdeepenings beneath the Antarctic and Greenland ice sheets using a GIS-based algorithm that identifies closed-contours in the bed topography and then describe and analyse the characteristics and metrics of a subset of overdeepenings that pass further quality control criteria. Overdeepenings are found to be widespread, but are particularly associated with areas of topographically laterally constrained ice flow, notably near the ice sheet margins where outlet systems follow deeply incised troughs. Overdeepenings also occur in regions of topographically unconstrained ice flow (for example, beneath the Siple Coast ice streams and on the Greenland continental shelf). Metrics indicate that overdeepening growth is generally allometric and that topographic confinement of ice flow in general enhances overdeepening depth. However, overdeepening depth is skewed towards shallow values – typically 200–300 m – indicating that the rate of deepening slows with overdeepening age. This is reflected in a decline in adverse slope steepness with increasing overdeepening planform size. Finally, overdeepening long-profiles are found to support headward quarrying as the primary factor in overdeepening development. These observations support proposed negative feedbacks related to hydrology and sediment transport that stabilise overdeepening growth through sedimentation on the adverse slope but permit continued overdeepening planform enlargement by processes of headward erosion.

1. Introduction

Closed topographic depressions in the beds of present and former ice masses – also known as 'overdeepenings' – are an implicit feature of glaciated landscapes (e.g. Linton, 1963; Cook and Swift, 2012). Arguably, process understanding of overdeepening formation and significance has been disadvantaged by an absence of quantitative empirical studies of their distribution and morphology (Cook and Swift, 2012; Patton et al., 2015), which contrasts sharply with the availability of empirical data for other subglacial phenomena, such as drumlins (Clark et al., 2009). Awareness of this landform type is growing, most notably because the reverse-bed gradients created by overdeepenings are known to reduce subglacial drainage system transmissivity (e.g. Creyts and Clarke, 2010), thus affecting ice-bed coupling and basal sliding, and known to dispose marine-terminating outlet glacier systems to rapid, episodic retreat (e.g. Weertman, 1974; Thomas, 1979; Jamieson et al., 2012; Nick et al., 2009; Schoof, 2007). In addition, the amplitude and wavelength of subglacial topography is fundamental to the rate of glacier sliding because basal drag is sensitive

* Corresponding author.
E-mail address: d.a.swift@sheffield.ac.uk (D.A. Swift).
[1] Present address: CAGE—Centre for Arctic Gas Hydrate Environment and Climate, Department of Geology, UiT The Arctic University of Norway, 9037, Tromsø, Norway.

http://dx.doi.org/10.1016/j.quascirev.2016.07.012

to obstacle scale and, in particular, slope (Schoof, 2005). A dearth of empirical data not only hampers our ability to build generalised views of overdeepening origin and evolution, but also our ability to develop and test numerical models that couple glacial and landscape processes.

Overdeepenings are found in a wide variety of contexts, including glacier troughs and trough confluences (Fig. 1A&B), and beneath glacier and ice stream termini (Fig. 1C; Haeberli et al., 2016, Table 1 in Cook and Swift, 2012). The origin of these features has been debated widely. The focussing of ice flow, which can occur in troughs and especially at trough confluences, has been shown theoretically to increase erosion potential (e.g. Anderson et al., 2006; Kessler et al., 2008; Lloyd, 2015). However, the occurrence of overdeepenings in other contexts has focussed attention on the possibility of independent positive feedbacks that promote focussed, deep erosion of the bed (illustrated in Fig. 2) (Cook and Swift, 2012). Hooke (1991) proposed that overdeepenings might initiate because bed irregularities cause crevassing at the ice surface that should enhance the quarrying rate at these locations via the delivery of large volumes of surface melt to the bed. Hooke (1991) further proposed that amplification of the irregularity would further enhance the quarrying rate. Others (e.g. Alley et al., 1997; Herman et al., 2011) have emphasised enhanced erosion in the ablation zone driven by abundant surface melt motivating fast glacier sliding and fluvioglacial sediment flushing. Chains of overdeepenings have been suggested to arise from lithological variabilities that produce suitable initial bed irregularities (e.g. Glasser et al., 1998) but also wave-like instabilities in ice flow that should result in overdeepenings with regular spacing and amplitude (Mazo, 1989).

Overdeepenings are able to form in glacier and ice sheet beds because positive ice surface gradients permit ice and subglacial water to ascend adverse subglacial slopes. Evacuation of sediment by ice and water flow thus permits continued ice-bed erosion and therefore continued enlargement of the deepening basin. However, Shreve (1972) and Röthlisberger (1972) observed that adverse slopes impose limitations on the flow of subglacial water such that a hydraulically efficient channel that ascends an adverse slope that exceeds a threshold relation of around −1.6 times the ice surface slope will begin to close (the exact value is dependent on the parameters used; see Werder (2016)). Hooke (1991) proposed that this feedback should stabilise overdeepening development by restricting the transport of sediment by water and thus depositing a layer of till. Subsequent theoretical work (Alley et al., 1998, 2003; Creyts and Clarke, 2010) has supported the proposed importance of this feedback, and observations of overdeepening basal water pressures at near-overburden pressure (see Cook and Swift, 2012) support a switch in drainage transmissivity. Unfortunately, examination of the adverse bed slope to ice surface slope relation for Quaternary overdeepenings is unlikely to provide significant insight into their formation because (a) the ice geometry relevant to the period of formation cannot be known and (b) high water pressures and sediment deposition in overdeepenings reduces drag exerted by the bed (Cook and Swift, 2012), leading to a flattening of the ice surface above (cf. Haeberli et al., 2016). Further, theoretical work by Werder (2016) shows that the aforementioned threshold relation only represents the lower limit of the threshold at which channel closure occurs.

To stimulate new observational studies and the development of numerical ice-erosion models (e.g. Egholm et al., 2012), we present an overview of overdeepening distribution and morphology beneath the present ice sheets, and examine how large quantitative datasets on overdeepening characteristics might inform our understanding of overdeepening origin and evolution. To achieve this aim, we first use an automated GIS-based approach described by Patton et al. (2015) to map overdeepenings in published bed-topography datasets for Greenland and Antarctica, and then apply strict quality control criteria to the mapped dataset prior to the analysis of a range of overdeepening metrics. We do not map overdeepenings in formerly glaciated environments because post-glacial processes in these environments, such as sedimentation and lake formation, tend to obscure overdeepening depth and extent (e.g. Preusser et al., 2010). Analyses of mapped overdeepening distribution and morphology are used to explore (i) overdeepening

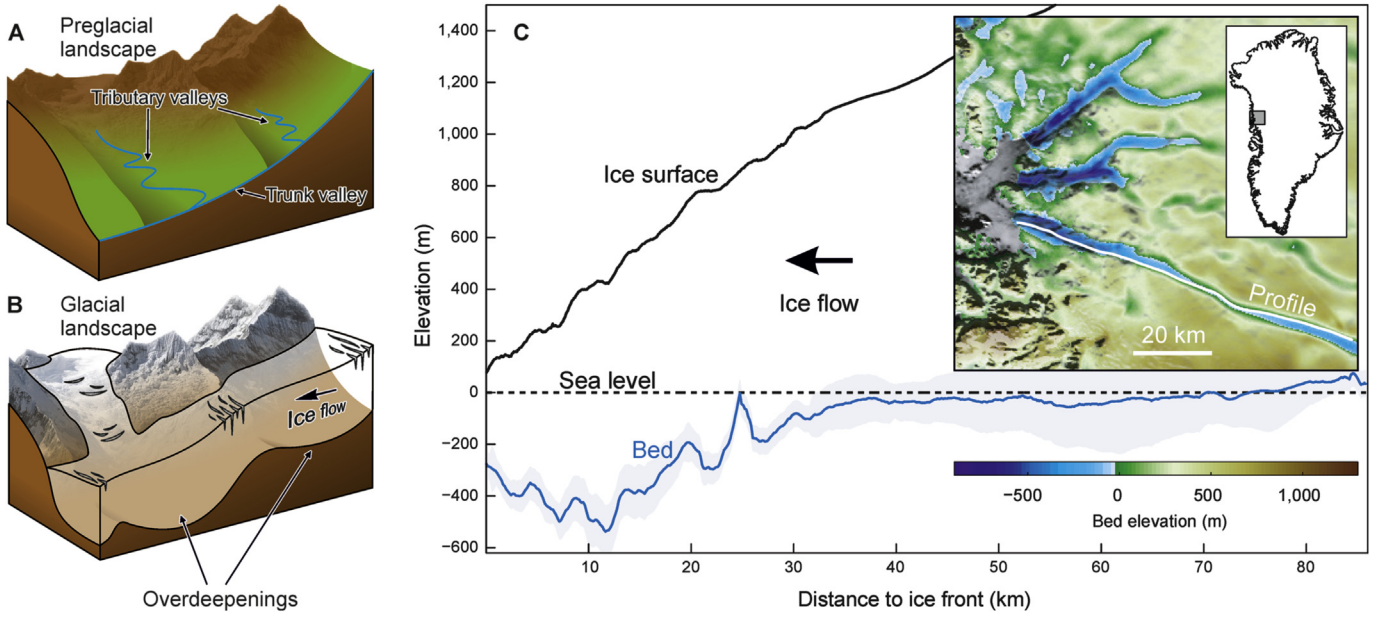

Fig. 1. Overdeepenings in valley glacier and in ice sheet outlet glacier contexts. A and B. Cartoon showing modification of a fluvial valley long-profile by glacial erosion, producing overdeepened basins. C. Overdeepenings in the bed of an outlet glacier in NW Greenland (redrawn from Morlighem et al., 2014). The location of the profile is shown in the inset. A large overdeepening extends some 30 km beneath the ice from the ice front and contains numerous 'nested' overdeepenings (the elevation axis is greatly exaggerated to show the bed topography).

Table 1
Number and area of depressions in Antarctica and Greenland.

	Antarctica			Greenland		
	$km^2 \times 10^6$	Number	% of total	$km^2 \times 10^6$	Number	% of total
Total land area mapped (including shelf)	16.45	–	–	3.45	–	–
All depressions[a]	4.90	–	–	0.54	–	–
Mapped dataset (Fig. 4)[b]	3.02	9905	100	0.35	3948	100
- Parent depressions only	As above	6290	63.5	As above	2663	67.5
- Parent depressions containing nested depressions	–	2536	25.6	–	968	24.5
Metric dataset (Fig. 6)[c]	–	764	12.1	–	335	12.6
- Topographically confined only	–	367	5.8	–	111	4.2
Metric dataset by ice sheet thermal regime						
- Warm (cold) depressions only	–	225 (162)	–	–	n/a	–
- Topographically confined warm (cold) depressions only	–	52 (106)	–	–	n/a	–

[a] Includes tectonic depressions (i.e. with perimeters >2000 km; see text); not quality controlled.
[b] Excludes tectonic depressions and depressions that do not meet other mapping criteria (see text); includes nested depressions.
[c] Excludes nested depressions, depressions that are not elongate in the ice flow direction, and depressions that do not meet other quality control criteria (see text).

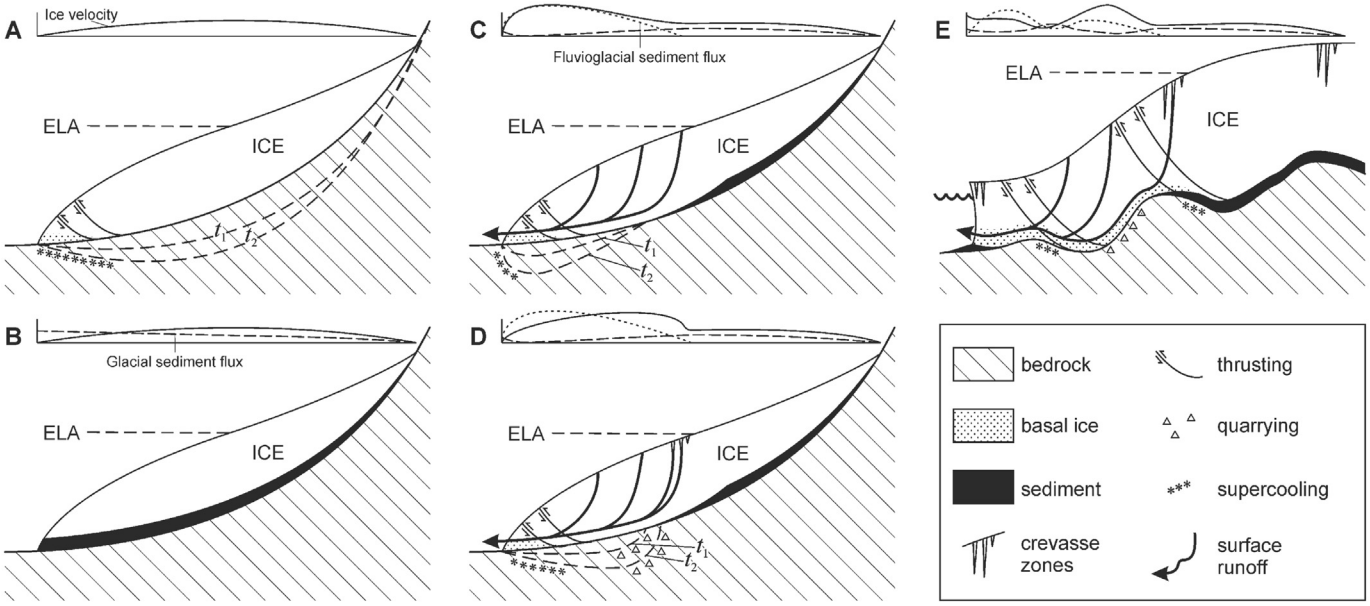

Fig. 2. Schematics summarising key processes likely involved in overdeepening initiation and growth (redrawn from Cook and Swift, 2012). Each schematic shows ice thickness and bedrock topography along the glacier centre-line and it is assumed that there are no tributaries or confluences. Ice flow is right-to-left and dashed lines below the glacier bed indicate time horizons during evolution of the bed. Graphs inset above each schematic indicate relative ice velocity and (where relevant) the flux of sediment in glacial versus fluvioglacial pathways. A. Glacier mass balance requires that ice velocity should vary down glacier, and should peak roughly beneath the equilibrium line (EL); if glacial erosion scales with velocity, this is where overdeepening might be expected. B. Without sufficient sediment evacuation, erosional products would accumulate and protect the bed, causing erosion to cease. C. The importance of sediment flushing by subglacially routed surface melt predicts that erosion potential is low beneath the accumulation area and then increases rapidly downglacier of the EL because the flux of subglacial meltwater increases. This suggests a downglacier-shift in the locus of overdeepening. D. Hydrological and ice velocity feedbacks (see main text) predict that erosion should be promoted at the overdeepening head and discouraged on the adverse slope, leading to an asymmetric overdeepening form that is deepest near the overdeepening head. E. Multiple overdeepenings and complex spatial patterns of erosion beneath an outlet glacier system resulting from variation in climate and lithology (see Cook and Swift, 2012).

distribution and size, including differences between the Greenland and Antarctic ice sheets that may reflect climatic influences or glacial history, (ii) overdeepening morphology, and (iii) controls on overdeepening size and depth, including the influence of topographic focussing of ice flow. Our approach yields several important insights and these are used to propose a conceptual model of overdeepening formation that may be a useful challenge for ice-erosion models.

2. Methods & data

Automated GIS methods (Patton et al., 2015) enable rapid and objective delineation and classification of closed topographic depressions in very large bed-topography datasets and subsequent extraction of metrics that describe overdeepening form. Nonetheless, the level of insight that can be acquired using such approaches is clearly limited by the quality of metrics that the source datasets permit, meaning strict quality control methods (Patton et al., 2015) were also applied.

2.1. Overdeepening delineation

Given that the glaciological parameters necessary for the creation of overdeepenings are unknown, and given that existing forms may be relict or actively evolving, the approach taken was to identify and map overdeepenings based purely on the morphological expression of the bed topography. GIS-based 'fill' tools offer a convenient means of mapping closed depressions in a landscape,

but these miss smaller features that are nested within larger glacial or non-glacial basins. The method of Patton et al. (2015) therefore delineates overdeepenings using a GIS-based algorithm that tracks changes in contour length with distance from initial points of elevation minima (Fig. 3). A sudden increase in contour length indicates when a closed depression has been breached, and the method enables one to use contour-length to set minimum and maximum limits on overdeepening size. An increase in contour length of >90%, which indicates at least a doubling of the depression area, was determined to be an appropriate threshold for defining the depression perimeter (Patton et al., 2015). By running the algorithm iteratively, enclosed (nested) depressions can be mapped (Fig. 3B). Depressions are categorised into 'parent' and 'child' types, with nesting order determined by lip elevation (Fig. 3C).

2.2. Overdeepening metrics and adverse slope to surface slope relation

Automated methods (Patton et al., 2015) were used to extract information on overdeepening size and form (Fig. 3D), including length, width, and long- and cross-profiles that pass through overdeepening elevation minima (i.e. deepest points) between depression entry and exit points. Depth was measured relative to the overdeepening exit point (i.e. lip). Entry and exit points were identified using the maximum and minimum ice-surface elevation points that lie above the bounding contour of the depression, and the long-profile was determined by calculating the 'least-cost' (i.e. deepest) path that connects the in- and outflow points to the elevation minimum. This approach is suitable for both linear and sinuous or curving overdeepenings where the deepest route through the depression is not a straight line. Because ice and water flow are guided strongly by bed topography, this path should approximate closely the route taken by ice, water and sediment at the ice sheet bed. The adverse slope to surface slope relation was determined using the gradient between the overdeepening deepest point and lip and that of the overlying ice surface, the lip position being determined from available data on present ice sheet topography (see below). Thus, following Werder (2016), we use the mean surface and bed gradient over the whole of the adverse slope. The

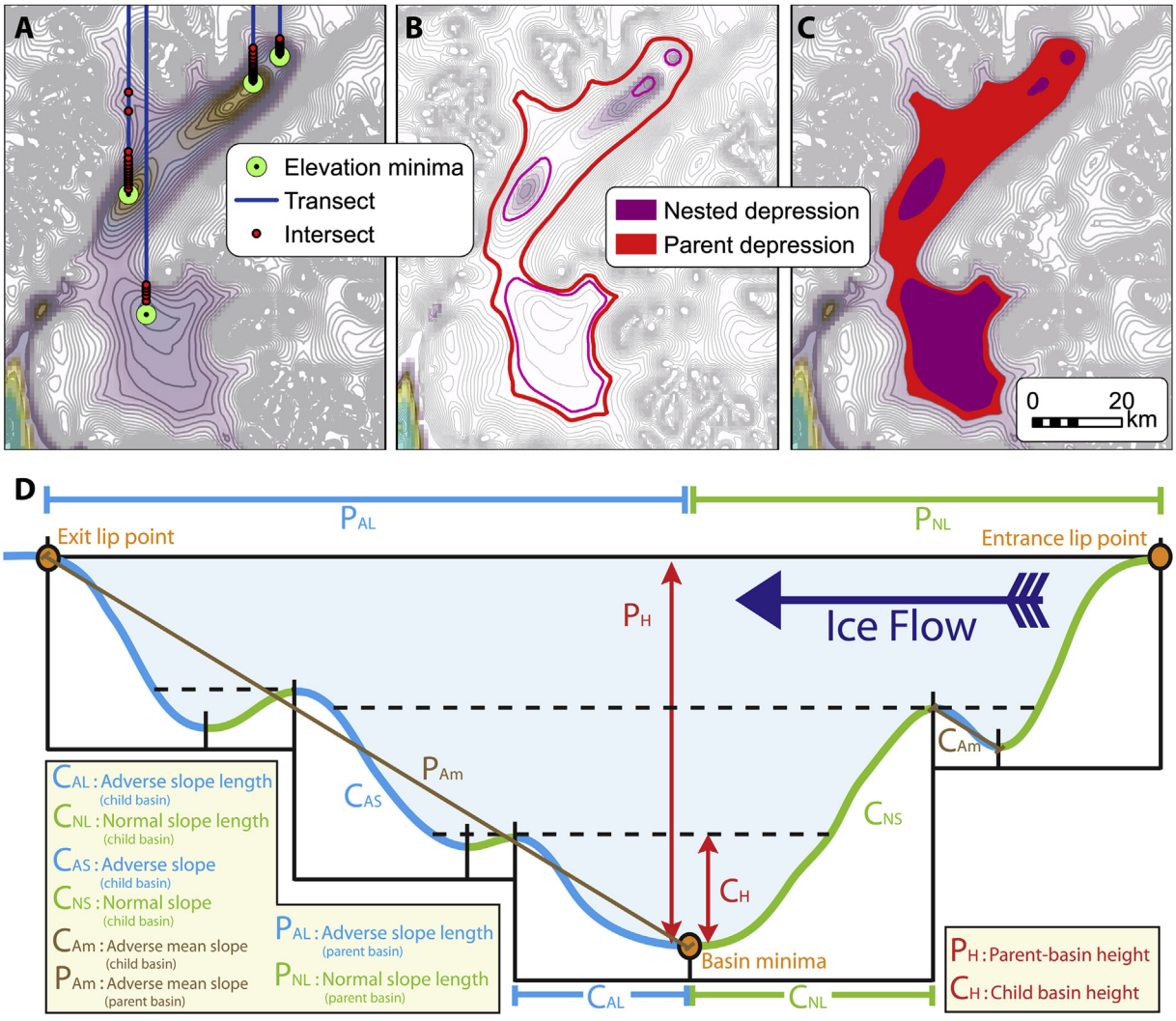

Fig. 3. A–C. Contour-tracking method used to identify nested depressions from a digital elevation model. Source: Patton et al. (2015). First, elevation minima were found by applying a zonal statistical tool to areas of depression-like topography identified using a terrain analysis mask. Second, depression perimeters were determined by measuring the change in contour length between successive contours encountered along a linear transect starting at each elevation minimum. Contour lengths along the transect increase in size gradually inside the depression and increase rapidly when the depression lip is 'breached'. D. Cartoon showing the long-profile of a subglacial 'parent' depression containing nested 'child' depressions. Various metrics that describe the form of the depression and associated child depressions are defined. Source: Patton et al. (2015).

resolution of the bed topography datasets does not permit the calculation of meaningful values for this relation over shorter length scales.

2.3. Overdeepening shape and context

Overdeepenings typically develop elongate planforms, with the long-axis oriented in the direction of ice flow (e.g. Cook and Swift, 2012). Depression shape and orientation with respect to ice flow direction were therefore used as a means to exclude non-glacial features or genuine overdeepenings that might have formed under previous ice sheet configurations and are therefore unlikely to be in equilibrium with present ice sheet parameters. To achieve this, 'circular' depressions were first identified. Next, the elongation of the remaining depressions was determined using the mean width of each depression, where width is measured perpendicular to the least-cost path at intervals along the long-profile. Depressions were classified as 'elongate' where their long-profile length exceeded the mean width by a factor of two. Additionally, because overdeepenings are typically found in areas of focused glacial erosion characterised by trough and fjord incision (Cook and Swift, 2012), depressions were also classified as 'topographically confined' where the mean relief within a small (20 km) buffer of the depression perimeter was found to exceed 500 m (cf. Patton et al., 2015).

2.4. Study areas, data sets, and quality control

Current bed-topography datasets for Greenland (Bamber et al., 2013) and Antarctica (Fretwell et al., 2013) are the products of gridded interpolations between spatially heterogeneous measurements of ice thickness obtained from a variety of sources (Fig. S1 A&B). Further, these datasets also include topography in adjacent non-glaciated areas that are also derived from a variety of topographic and bathymetric sources. The quality of the resulting bed-topography datasets is therefore highly variable spatially, and mapped features require robust scrutiny. Alternative bed-topography datasets derived using mass conservation are available (e.g. Morlighem et al., 2014) but at present the ability to resolve bed topography with suitable accuracy using this method is limited to fast-flowing glacier systems near the ice sheet peripheries.

2.4.1. Antarctica

The Bedmap2 data set (Fretwell et al., 2013) uses ice-thickness measurements derived from a variety of sources, including: direct airborne radar sounding and seismic measurements; satellite altimetry and free-air gravity surveys; and a 'thin-ice' model for thinly glaciated areas near the ice-sheet margin. The Bedmap2 topography is provided as a 1 km grid but measurements of ice thickness were sampled at 5 km, primarily because the distribution of empirical measurements did not warrant a higher resolution (Fretwell et al., 2013). Nonetheless, spatial uncertainty remains significant at a 5 km resolution, with only 33% of cells containing direct data measurements. Absolute uncertainty in subglacial bed elevation varies between ±66 to ±1008 m.

2.4.2. Greenland

The Greenland dataset (Bamber et al., 2013) is again provided as a 1 km grid, with data sources similar to those for the Bedmap2 dataset, though levels of absolute uncertainty in subglacial bed elevation are slightly lower at 0–150 m. Onshore data are merged with the most recent IBCAO (International Bathymetric Chart of the Arctic Ocean) dataset (Jakobsson et al., 2012). However, poor data coverage within fjordal zones results in fjord-bed elevations near glacier grounding-lines being underestimated by up to several hundred metres (e.g. Rignot et al., 2015).

2.4.3. Quality control

Two levels of quality control were implemented for this study:

- Overdeepening mapping: Criteria (Patton et al., 2015) were applied to the mapping of depressions, both on and offshore (see Section 3.1), to prevent delineation of artefact depressions produced by the interpolation method (kriging), as well as to exclude small depressions beyond areas of suitable data coverage. As a result, the mapped dataset constitutes only depressions with: (1) a minimum depth of 40 m; (2) a maximum perimeter of 2000 km, to exclude tectonic basins; and (3) a minimum adverse slope length of 5 km, the resolution of the Bedmap2 data (above).
- Overdeepening morphology: Metrics (see Section 3.2) were obtained only for mapped depressions classified as elongate (see above), meaning that this dataset was, by nature, restricted to depressions in subglacial locations where information on ice flow direction was available. In addition, to ensure high dataset quality, metrics were not obtained for: (1) depressions for which the mean flightline density (Fig. S1C&D) over the entire depression fell below 0.11 lines per km; and (2) nested depressions lying inside parent depressions. Hence, these depressions occur only in the mapped dataset. Within the metric dataset is the subset of depressions classified as topographically confined.

2.4.4. Ice velocity data

Ice-surface velocity data required for evaluation of overdeepening elongation with respect to ice flow direction (above) was sourced from Rignot et al. (2011) and Joughin et al. (2010) for Antarctica and Greenland, respectively.

3. Results

3.1. Number and distribution of potential overdeepenings

The mapped dataset (Fig. 4) comprises depressions in both subglacial and submarine contexts. Statistics derived from the mapped dataset (Table 1) indicate that ~18% of the Antarctic and ~10% of the Greenland continental and shelf areas are overdeepened and that there may be as many as 9905 individual subglacial overdeepenings in Antarctica and 3948 in Greenland. Unsurprisingly, depression distribution to some extent reflects the density of ice-thickness measurements. For example, in Antarctica, higher measurement densities over Marie Byrd Land, in the Gamburtsev Mountains, and in the Lambert Glacier catchment produce significantly more depressions (Fig. 4A) than in other interior areas of the East Antarctic ice sheet. Furthermore, depressions appear to be less frequent beneath the major ice shelves in Antarctica as a result of poor bathymetric constraints in these areas (Fretwell et al., 2013; Timmermann et al., 2010). In Greenland, the greater number of depressions mapped within the Jakobshavn Isbræ catchment (Fig. 4B) reflects the dense array of ice-thickness measurements here (Fig. S1). Conversely, there is a notable absence of depressions in some fjordal regions, especially to the north of Uummannaq Fjord in the West and to the south of Ammassalik Island in the East, where incorrect fjord bed elevations (see 2.4.2) have been adjusted manually (Bamber et al., 2013) to match ice thickness-derived ice-bed elevations.

'Tectonic' depressions (i.e. those with perimeters >2000 km) are shown in Fig. 5. These are associated with known rift systems, or, in Greenland, with the isostatically depressed landscape beneath the

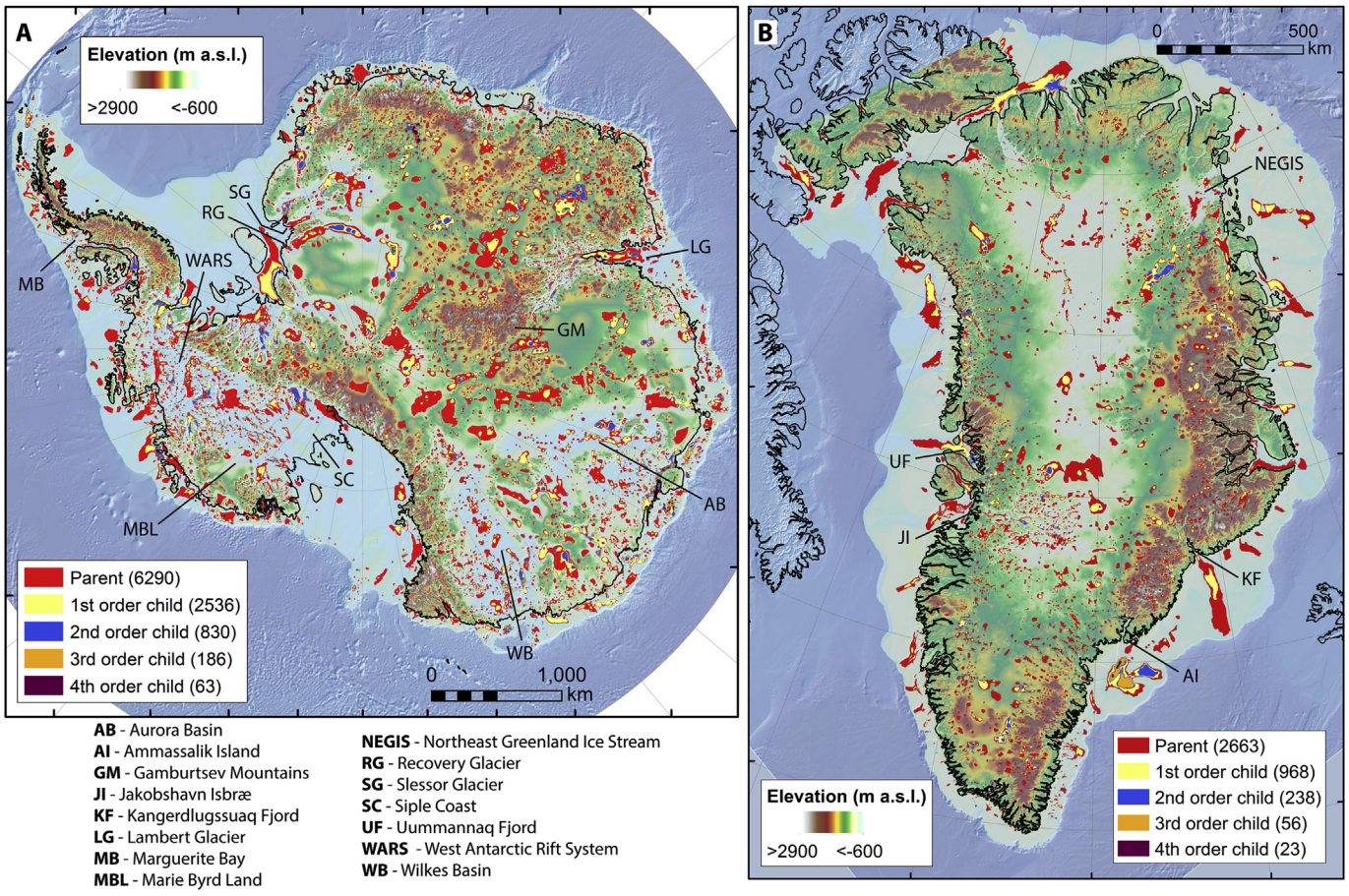

Fig. 4. Closed depressions and their nestings in (A) Antarctica and (B) Greenland. A high-quality version is available as supplementary information (Figure S3).

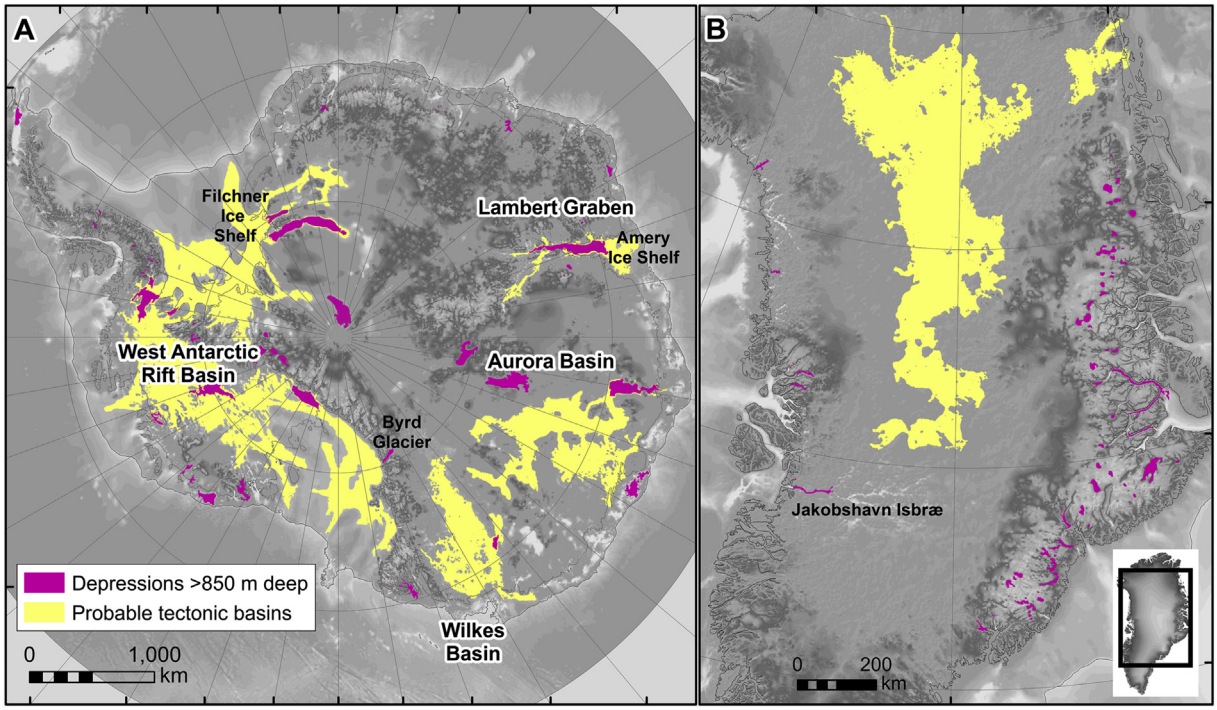

Fig. 5. Probable tectonic basins (i.e. with perimeter >2000 km) across Antarctica (A) and Greenland (B). Depressions smaller than the tectonic threshold but deeper than 850 m are marked in pink and, in Antarctica, these are closely associated with rift basins. (For interpretation of the references to colour in this figure legend, the reader is referred to the web version of this article.)

centre of the ice sheet (Fig. 5B). In Antarctica, these depressions are associated with the West Antarctic Rift System and smaller Lambert Graben, as well as with two large extensional basins, the Wilkes and Aurora Subglacial Basins (Fig. 5A). In Greenland, the second and smaller of only two large depressions occurs beneath the Northeast Greenland Ice Stream (Fig. 5B) in a geologically complex region situated on the western boundary of the Caledonian orogeny, which is an area subjected to extension during north Atlantic rifting (Strachan, 1994). These large depressions have undoubtedly been exploited and modified by flowing ice but are either known to have originated tectonically or are sufficiently large and complex such as to exclude a wholly glacial origin. It is notable that in Antarctica the majority of deep (>850 m) depressions are found within rift systems and their associated catchments (Fig. 5A), but in Greenland they occur mainly in the passively uplifted high-elevation East Greenland mountain range (Fig. 5B) (Swift et al., 2008).

The quality control criteria used to create the smaller metric dataset (Fig. 6) mean this sample represents only 12% and 3% of mapped depressions in Antarctica and Greenland, respectively (Table 1). Excluded are a large number of depressions that exhibit circular or complex morphologies that may be artefact depressions or real depressions that have evolved under former ice-sheet configurations when ice flow was inconsistent with that today. Remaining depressions are located predominantly in regions of medium to high relief where ice flow is directed along trough- and fjord-like valley systems that are indicative of glacial incision. These occur in the East Greenland mountain chain (Fig. 6B) and the Lambert Rift system, the Gamburtsev Mountains, and the West Antarctic Rift System (Fig. 6A), as well as in troughs that cross-cut high topography near the margins of both ice sheets, including the Transantarctic Mountains. This represents a common context for overdeepening formation (cf. Cook and Swift, 2012) and the context of high surrounding relief is further highlighted by a significant proportion of these features being classified as topographically confined (Table 1). A glacial origin for all these features is therefore highly probable. Other depressions are located in regions of lower relief in the ice sheet interiors that may not have a wholly glacial origin, but their concordance with present ice flow indicates that glacial modification is likely.

3.2. Size and morphology of overdeepenings

Key metrics derived from the 'overdeepening morphology' dataset are summarised in Fig. 7 (summary statistics are presented in Table S1). Full distributions of values for a variety of metrics are shown in Fig. 8 and relationships between various metrics are shown in Figs. 9 and 10.

3.2.1. General size and form

Dimensional statistics are dominantly positively skewed, with preferred (i.e. modal) and median values being typically lower than the respective mean values. The near-complete absence of depressions with width 0–2.5 km (Fig. 8B) and absence of those with lengths < 5 km (Fig. 8A) and depths <40 m (Fig. 8D) reflects our quality control criteria (above). Key observations include:

1. Preferred values for most metrics, including depth (Fig. 8D), elongation ratio (Fig. 8G), and asymmetry (Fig. 8E), are notably similar for Greenland and Antarctic overdeepenings.
2. Overdeepenings in Antarctica are slightly larger, notably in width (Fig. 8B), with mean values for length and width in

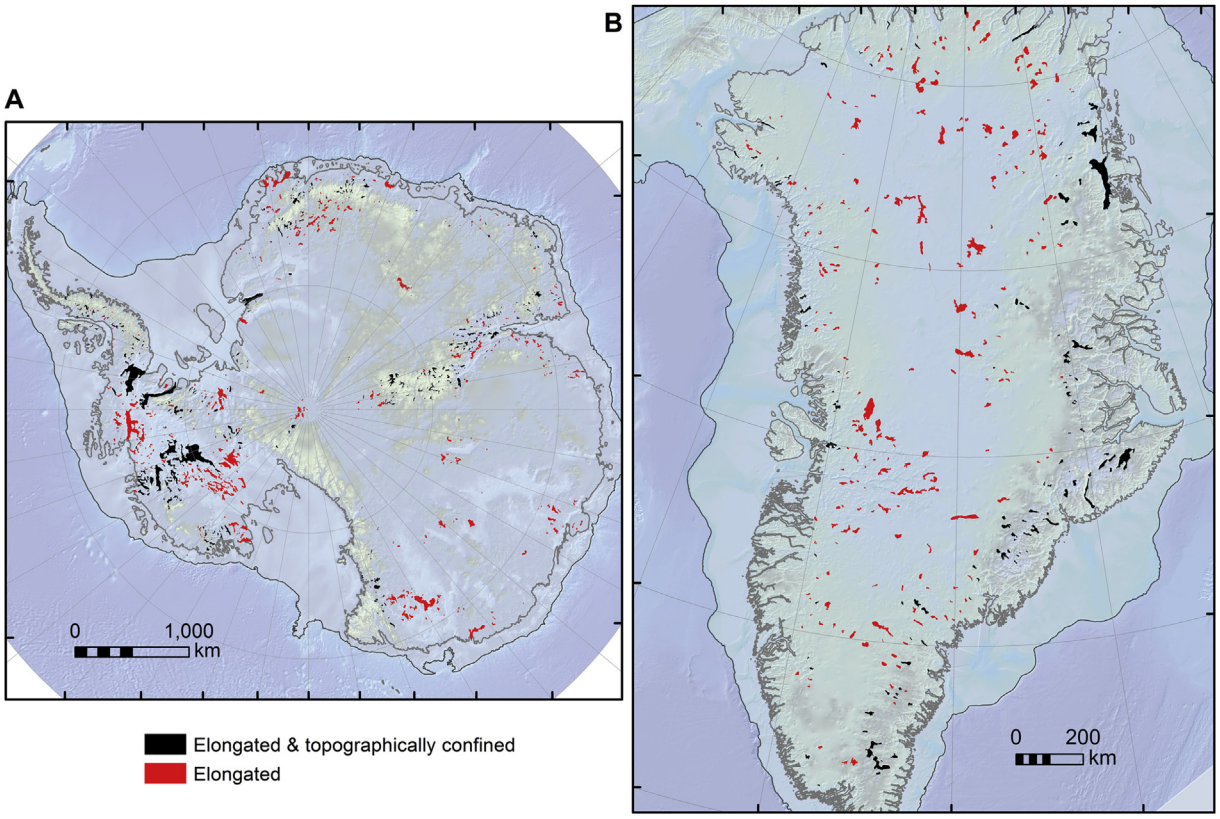

Fig. 6. Depressions used in the metric dataset. Black depressions are the subset classified as topographically confined (i.e. those depressions where the mean relief within a small (20 km) buffer of the depression perimeter exceeds 500 m; cf. Patton et al., 2015).

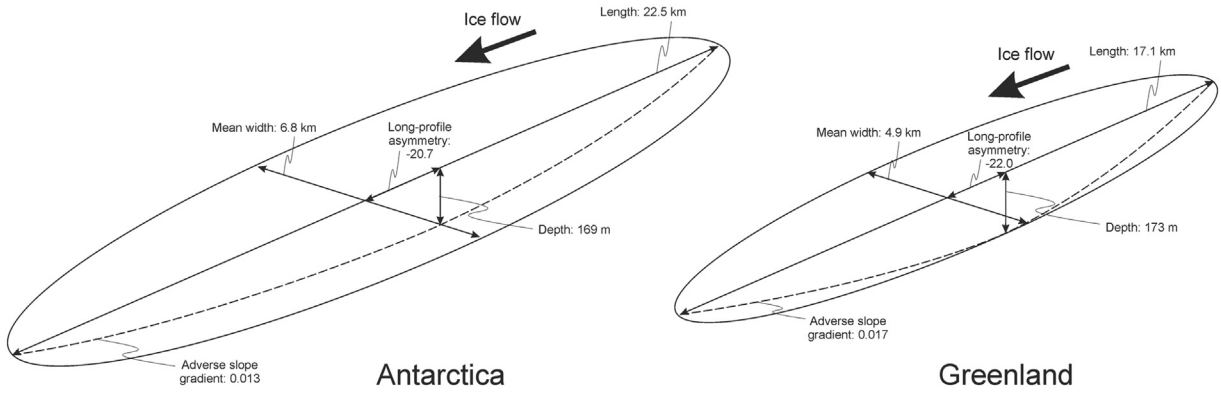

Fig. 7. Cartoons showing median measured values for overdeepenings in Greenland and Antarctica derived from the metric dataset. Dimensions are drawn to a relative scale and using 10× vertical exaggeration. See Table S1 for mean and standard deviation values.

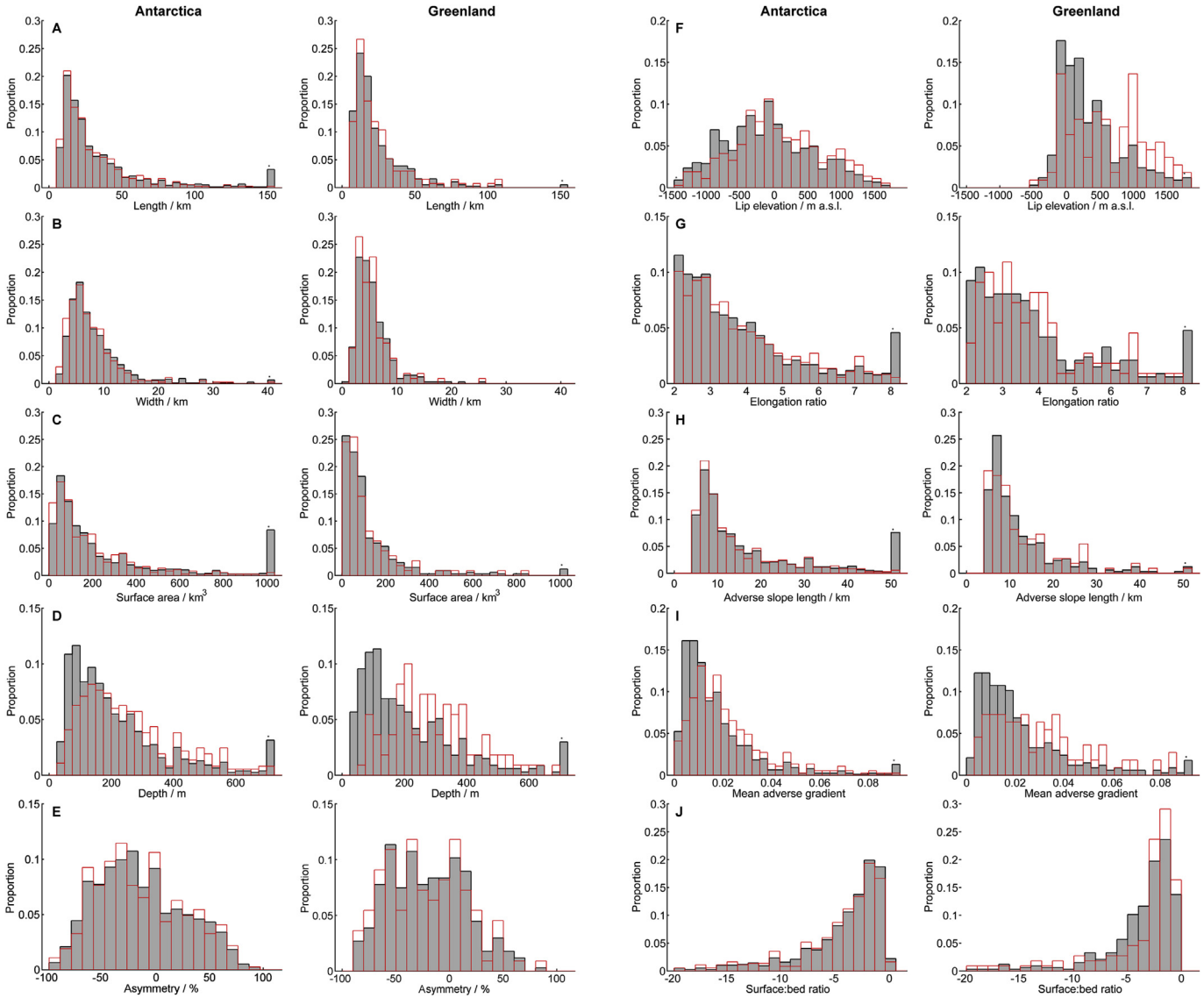

Fig. 8. Histograms showing the distributions of metrics for depressions that pass quality control criteria in Antarctica and Greenland. Red plots are for the subsets of overdeepenings that are classified as topographically confined. A star above the end bin indicates all data beyond this value are grouped into the final bin. (For interpretation of the references to colour in this figure legend, the reader is referred to the web version of this article.)

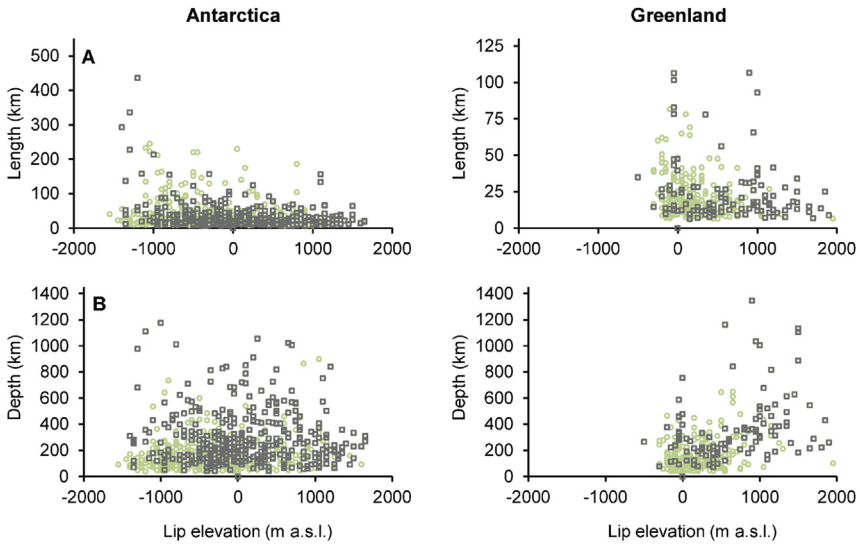

Fig. 9. Lip elevation distribution and relationship to A: length and B: depth. Grey symbols are for the smaller subset of topographically confined depressions.

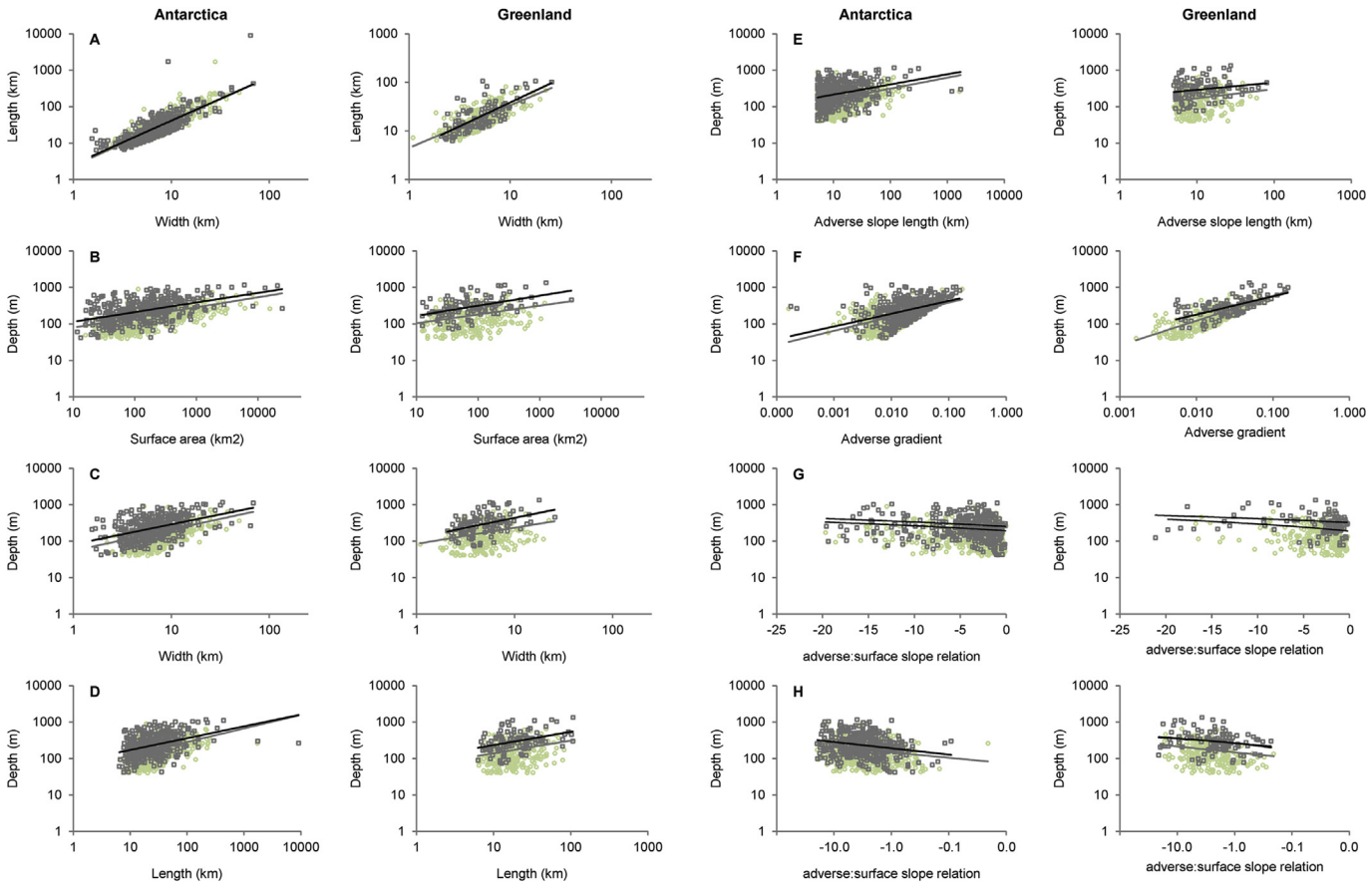

Fig. 10. Relationships between overdeepening width and length, and between various size metrics (surface area, width, length, and adverse slope length) and depth. Darker symbols show the relationship for the smaller subset of topographically confined depressions. All relationships are significant at $p < 0.05$ in log-log space. The darker fit-line indicates that topographically confined depressions are consistently deeper than non-confined depressions. In H the x-axis is shown on a non-log scale and the same data is shown in G using a log scale. Only the latter relationship was tested for significance.

Antarctica being around double those for Greenland, and median values are ~50% larger, respectively (Table S1).

3. Longest overdeepenings occurring close to sea level and length generally shortens with increasing lip elevation (Fig. 9A). Few overdeepenings exceed 100 km in length. Those exceeding this value occur largely in Antarctica in areas near the ice sheet margins.

4. Depth value distributions for both ice sheets are similar (Fig. 8D), with preferred depth being ~50–200 m (median ~170 m). Values exhibit a long tail, but only 8% and 7% of overdeepenings in Antarctica and Greenland exceed 500 m depth, respectively. There is no clear relation between depth and lip elevation (Fig. 9B), though topographically confined depressions in Greenland that are mainly located in areas of high elevation along the eastern coast (Fig. 6) exhibit deeper values than many that are at or near to sea level.
5. Overdeepening frequency in general diminishes with altitude (i.e. lip elevation; Fig 9A). In Greenland 77% of overdeepenings occur at or above sea level, whereas 60% in Antarctica are at or below sea level, including a great many located in the West Antarctic Rift System (Fig. 4).

3.2.2. Allometry

Elongation value distributions for Antarctica and Greenland are similar (Fig. 8G): median values are ~3.3–3.4 (Table S1) and few overdeepenings have extreme values. Scatter plots (Fig. 10) thus show strong correlation between overdeepening length and width (Fig. 10A). Correlation between depth and other measures of overdeepening size (Fig. 10B–H) is weaker but all correlations are significant (Table S3). Notably, best-fit lines for relationships between depth and many other variables (Fig. 10) (excluding total length and adverse slope gradient; Fig 10D&F) shows that the topographically confined subset of overdeepenings is consistently deeper than those classified as unconfined.

3.2.3. Profile asymmetry

Asymmetry is here reported as the relative position of the deepest point on the long profile, where 0 is the mid-point of the long-profile, −100% is the inflow point (or overdeepening 'head'), and +100% is the outflow (i.e. lip). A value of −50% indicates that the overdeepening is asymmetric, with the deepest point situated midway between the inflow point and the profile midpoint. Values for Antarctica and Greenland show that the deepest point is most commonly skewed towards the overdeepening head (Fig. 8E), though asymmetry is greater in Greenland, with median values being −20.7% and −22.0% for Antarctica and Greenland, respectively.

3.2.4. Adverse slope and the adverse slope to surface slope relation

Adverse slope length distributions show no preferred peak (Fig. 8H), being curtailed at 5 km as a result of the quality control criteria. Distributions for adverse slope gradient and the adverse slope to surface slope relation nevertheless show clear preferred peaks (Fig. 8 I&J). The preferred peak in adverse bed gradient for Antarctica is at a slightly shallower gradient than for Greenland (Fig. 8J), and for both ice sheets the gradient is steeper for overdeepenings classed as topographically confined (Fig. 8I) (see below). However, preferred adverse slope to surface slope relation values demonstrate the reverse pattern, with a slightly higher relation being preferred for Antarctica (approximately −2 to −3) than in Greenland (approximately −1 to −1.5) (Fig. 8J). Both settings show a sudden decline in adverse slope to surface slope relation values at −3 (Fig. 8J) that is particularly notable for Greenland.

3.2.5. Topographic confinement

Topographically confined depressions are skewed towards deeper values (Figs. 8D and 10). Preferred values are 175–400 m for Greenland (median 296 m) and 100–350 m for Antarctica (median 233 m) (Table S1). As a result, they typically have steeper adverse slopes (Fig. 8I), with Greenland examples exhibiting the steepest slopes. Nevertheless, topographically confined overdeepenings exhibit the same preferred adverse slope to surface slope relation as their non-confined counterparts (Fig. 8J).

3.2.6. Thermal regime

Erosion by cold-based ice is improbable but overdeepenings are found beneath areas of the Antarctic ice sheet that presently meet this condition (as mapped by Pattyn (2010); see Fig. S2). Such overdeepenings must have been formed during warmer conditions and have likely had less time to evolve than those in other areas. Depressions that do not lie entirely within areas of cold or warm bed regime were excluded. Distributions of metrics for those that remain exhibit some differences in preferred values (Fig. 11; Table S2), and these indicate that depressions under warm-based ice are deeper and possibly shorter with slightly steeper adverse-slope gradients. A notable difference in preferred lip elevation (Fig. 11D) predictably shows that cold-based areas are typically located at higher elevations where ice is thinner.

3.2.7. Ice sheet-specific similarities and contrasts

Median values show that overdeepenings, on average, are notably longer in Antarctica (~23 km) than Greenland (~17 km), and are also wider (at ~ 7 km versus ~ 5 km, respectively) (Table S1; Fig. 7; Fig. 8A and B). In addition, Antarctic overdeepenings also exhibit a more pronounced 'tail' of values with widths greater than 15 km, and surface area values are generally larger as a result (Fig. 8C). However, depths and adverse slope gradients are similar for the two ice sheets (Fig. 8D), except for a slight skew toward steeper gradients (Fig. 8I) in Greenland due to their generally smaller planform size (above). Preferred lip elevation is similar for both ice sheets at around −100 to 200 m, though Antarctica shows a second preferred lip elevation at ~ −400 to −500 m a.s.l. (Fig. 8A).

4. Discussion

4.1. Overdeepening distribution

The mapped set of depressions (Fig. 4) shows that overdeepening is widespread in both Antarctica and Greenland, and indicates that they occupy several common landscape or ice sheet contexts.

1. Depressions are associated with trough systems that dissect high topography near ice sheet margins. There are abundant examples on the east and west margins of Greenland (Fig. 4A), and in Antarctica. Notable examples in Antarctica are the Recovery Glacier and Slessor Glacier troughs and troughs crossing the Transantarctic Mountain chain (Fig. 4B).
2. Depressions are associated with major outlet glacier and ice stream systems that extend deep into the ice sheet interiors but are not necessarily in regions of high topography. For example, numerous individual depressions occur beneath Jakobshavn Isbræ and its tributaries in western Greenland (Fig. 4A), and in the Lambert and Siple Coast regions of Antarctica (Fig. 4B).
3. Depressions occur in palaeo-trough systems in the interior regions of the ice sheets. Notable examples occur in Antarctica within the Gamburtsev Range and the highlands surrounding the Aurora subglacial basin (Fig. 4B). Some examples are also found in central East Greenland (Fig. 4A) in troughs that may have been active at a time in ice sheet history when ice flowed to the west from a smaller ice sheet situated on the East Greenland Mountains.
4. Depressions are present within the interior of the ice sheets in areas of low relief and low elevation, which in Antarctica includes depressions within major 'tectonic' subglacial basins,

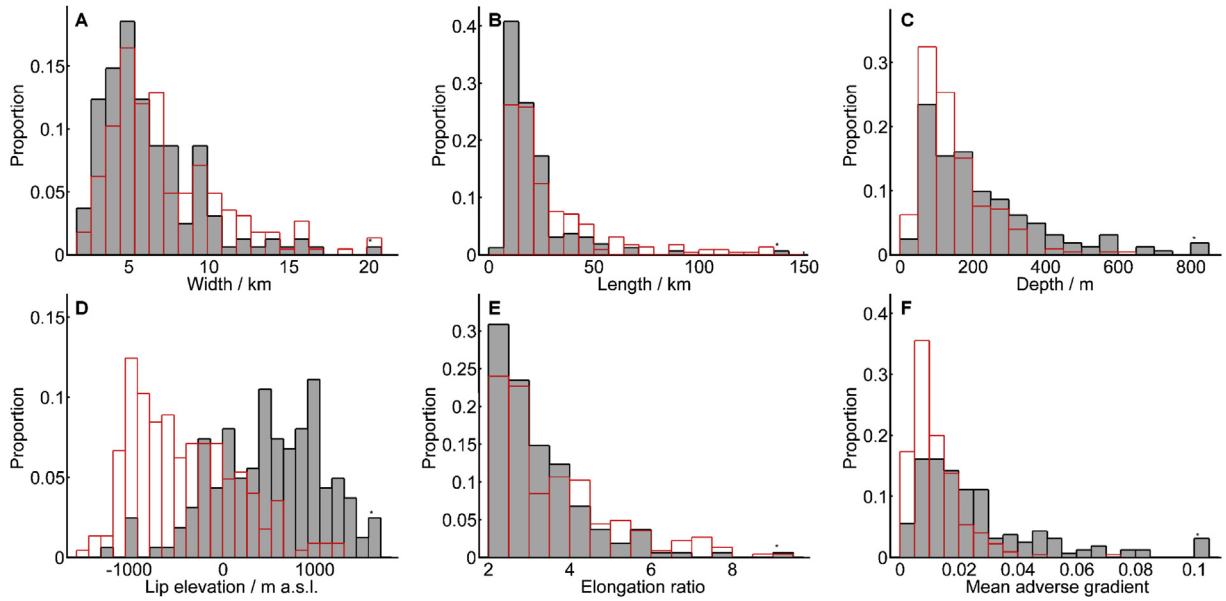

Fig. 11. Distributions of metrics for Antarctic overdeepenings classified according to modelled subglacial temperature regime. Red: overdeepenings in cold-based thermal regimes; Grey: overdeepenings in cold-based thermal regimes. (For interpretation of the references to colour in this figure legend, the reader is referred to the web version of this article.)

such as the Wilkes Basin, and within the deep topography of the West Antarctic Rift System that lies beneath the marine West Antarctic Ice Sheet, particularly so beneath ice inland from the Siple Coast area (Fig. 4B).

5. A number of major cross-shelf depressions occur beyond the present Greenland ice sheet limit. These extend from the mouths of notable fjord systems, including Uummannaq Fjord in the West and Kangerdlussuaq Fjord in the East (Fig. 4A) (cf. Batchelor and Dowdeswell, 2014). Examples are also present in Antarctica, including Marguerite Bay (Livingstone et al., 2012) Fig. 4B).

The association of overdeepenings with topographically constrained outlet-glacier systems and their tributaries is common in palaeo ice sheet contexts (e.g.Cook and Swift, 2012). The location of such systems probably reflects the location of pre-existing fluvial drainage systems that steered initial ice flow and became deeply incised as a result of erosion-steering feedbacks (e.g. Jamieson and Sugden, 2008; Kessler et al., 2008; Thomson et al., 2013). However, overdeepenings in Antarctica and Greenland are also frequent in interior basins and offshore shelf areas. Those in interior basins, particularly in Antarctica, include many examples where topographically confined ice flow may have occurred at or near the margins of smaller ice sheet configurations during earlier ice sheet history (e.g. Young et al., 2011), and such types can be produced by simple numerical ice-erosion models (e.g. Herman et al., 2011; Kessler et al., 2008). Other examples, including those offshore, indicate formation beneath areas of diffluent ice flow, or at least flow under very little topographic constraint, many of which appear to have been the location of fast-flowing palaeo ice streams. Notable examples are those on the Greenland shelf (Fig. 4A), including a highly elongate cross-shelf overdeepening at Kangerdlugssuaq fjord in southeast Greenland, and within and inland of the Siple Coast area of Antarctica (Fig. 4B). These 'diffluent' overdeepenings are difficult to reproduce in current ice-erosion models (e.g. Egholm et al., 2012) and indicate that positive feedbacks can sustain focussed erosion even where obvious lateral topographic constraints are absent.

Other key controls are likely to be thermal regime, crustal structure and lithology because these influence the efficacy of subglacial erosion processes. As observed above, overdeepenings in cold-based regions probably developed during warmer periods in ice sheet history. Crustal structure and lithology is likely to influence trough and overdeepening distribution through the presence or otherwise of geological weaknesses and variation in rock strength (Glasser and Ghiglione, 2009; Swift et al., 2008). Deep depressions in Antarctica are particularly associated with rift systems, for example, beneath the Filchner Ice Shelf (Jordan et al., 2013), at Byrd Glacier (Stump et al., 2006) and the in Lambert/Amery system (Harrowfield et al., 2005) (Fig. 5A), which may indicate that overdeepening is most efficacious in areas of faulted bedrock (cf. Lloyd, 2015). In Greenland, whilst it is possible that the overdeepened Jakobshavn Isbræ fjord and catchment is somehow associated with transient Palaeocene rifting (cf. Lundin and Doré, 2005), the majority of the deepest depressions are instead located in areas of high elevation that are generally of resistant bedrock (Fig. 5B). Previous work has indicated that resistive bedrock leads to the erosion of narrower glacial troughs with deeper overdeepenings (Augustinus, 1992b; Swift et al., 2008), which may explain the concentration of deep overdeepenings in, for example, the Eastern Greenland Mountains.

4.2. Overdeepening morphology and evolution

4.2.1. General form

Relationships between depth and other measures of overdeepening size show substantial scatter (Fig. 10). This is consistent with the limitations of the source datasets (cf. Patton et al., 2015), and weaker relationships for Greenland depressions may reflect the limited sample size. Nonetheless relationships are statistically significant (Table S3) and indicate growth of overdeepenings is broadly allometric and preferred values indicate broadly similar morphologies. This indicates an intrinsically similar process of origin and evolution influenced by local environmental controls. Scatter and distribution plots indicate the influence of several local factors on overdeepening size:

1. Elevation. The hypsometry of the Antarctic landmass means pre-glacial (and therefore glacial) catchment sizes are larger than in Greenland. Also associated with larger catchment areas are larger U-shaped valley sizes (Augustinus, 1992a; Haynes, 1972) and longer trunk-valley systems that mean overdeepening growth may be less restricted in Antarctica. For example, many overdeepened Antarctic ice stream beds reach far into the ice-sheet interior (e.g. Le Brocq et al., 2008). Catchments at higher elevations are typically smaller and have less space to accommodate overdeepening growth, and are also likely to have lower ice fluxes.
2. Relationship to sea level. Deepening of depressions below sea level must at some point cease because the ice will approach floatation, thus preventing further erosion, and because, in successive glaciations, glacial conditions of a progressively greater intensity are required for ice to re-advance into and re-excavate the basin (cf. Cook and Swift, 2012). Plots of overdeepening length versus lip elevation (Fig. 9) certainly show that the longest overdeepenings are situated around sea level, implying that overdeepenings grow mainly by headward erosion when bed erosion reaches below sea level.
3. Topographic confinement. Confinement of ice flow appears to lead to greater overdeepening depth, whereas length and width appear unaffected (Fig. 8). This factor seems to be more influential for Greenland overdeepenings than for those in Antarctica. This suggests several possible mechanisms. First, it is possible that topographic focussing of ice flow is more effective at enhancing erosion in Greenland because of the increased sliding and flushing rates promoted by the penetration of surface melt to the bed (e.g. Zwally et al., 2002). Second, it is possible that lithological differences promote erosion of deeper troughs and overdeepenings in Greenland than in Antarctica (Augustinus, 1992b; Swift et al., 2008).
4. Thermal regime. There is a slight increase in depth of overdeepenings beneath warm-based ice in Antarctica (Fig. 11). This is consistent with the assumption that overdeepenings beneath cold-based ice have had less time for growth or that, when conditions favouring erosion do occur in these locations, they are less favourable than for other areas.

4.2.2. Interpretation of long-profile asymmetry

The potential process significance of overdeepening long-profile morphology has been highlighted by Cook and Swift (2012) because: (i) erosion by means of abrasion, which is enhanced by flushing and the accumulation of material for bedrock erosion, should be focussed toward the overdeepening lip; (ii) quarrying should be focussed at the overdeepening head (although abrasion is also likely to be important here too as a result of the local steepening of the bed profile; and (iii) deposition is more likely to occur on the adverse slope as a result of changes in drainage transmissivity, and this may stabilise adverse slope gradient (cf. Hooke, 1991).

Our relatively crude measure of overdeepening asymmetry indicates that overdeepening evolution by headwall erosion is predominant, either because positive feedbacks enhance erosion on the normal slope, or because negative feedbacks act to stabilise the gradient of the adverse slope. The former implicates quarrying (or at least headwall erosion) as the dominant process in overdeepening evolution. However, the quarrying related feedback envisaged by Hooke (1991) depends on surface melt, implying that Antarctic overdeepenings are relict features characteristic of a warmer climatic regime. An alternative mechanism is that localised steepening of the bed (cf. Herman et al., 2011) may enable abrasion to play a similar role in Antarctic overdeepening evolution, or it is possible that pressure reduction in the lee of the overdeepening head motivates quarrying here by stimulating refreezing of water moving subglacially, which may entrain sediment without limit (Hooke, R. LeB., pers. comm.). These alternative mechanisms indicate that it is stabilisation of the gradient of the adverse slope that is most important, and therefore support the existence of a threshold adverse slope to surface slope relation that results in sediment deposition on the adverse slope. Nonetheless, Fig. 12 shows that steepest adverse slope gradients occur in median-sized overdeepenings (e.g. by median length or width), and this indicates that overdeepening size in general, in addition to the threshold relation, may exert a control on depth (this is explored more fully below).

4.2.3. Interpretation of the controls on overdeepening depth

The preference for relatively shallow overdeepening depths (Fig. 8D) implies that few overdeepenings attain maximum possible depths. There are several possible explanations for this that relate to the timing and mechanisms of overdeepening initiation. First, abundant small depressions may represent relict landforms that relate to periods of 'minimum' glaciation, and have been subsequently preserved under areas of non-erosive ice. This is unlikely, though, because overdeepenings in trough contexts, where rates of glacial erosion are high, constitute the majority of overdeepenings in the dataset. Second, it is possible that there has not been sufficient time. This also unlikely because of the location of many overdeepenings in troughs where process rates should be relatively high. Third, overdeepenings could arise from an instability in ice flow, as envisaged by Mazo (1989), meaning overdeepenings may be a feature of the glacier beds in much the same way as pool-riffle sequences occur in fluvial beds, and these may migrate down- or up-flow, with larger examples only occurring in rare circumstances where other notable feedbacks are present. Fourth, ice-bed irregularity feedbacks (Hooke, 1991) may lose their efficacy as overdeepenings become larger, such that minor bed irregularities are enhanced in preference to larger, existing overdeepenings.

More plausible explanations relate to the possibility that the rate of growth of overdeepening depth slows over time as a result of negative feedbacks. Strong preferred values for the adverse slope to surface slope relation (Fig. 8J) indicate a possible control on overdeepening depth imposed by the proposed switch in drainage transmissivity that occurs when this relation exceeds a threshold. However, preferred values exhibited by our dataset are larger than the 'classic' threshold of −1.6, and many values greatly exceed this threshold. Such values are permissible using the modified relation presented by Werder (2016), which corrects for water pressure below overburden downstream of the overdeepening lip, but the validity of this assumption in the context of Antarctic overdeepenings is unclear: Antarctic subglacial drainage morphology remains poorly understood, and the absence of surface melt, and the prevalence of marine ice-margins, implies that drainage is predominantly distributed and that basal water pressures are not widely below overburden. In addition the usefulness of the adverse slope to surface slope relation for understanding overdeepening initiation and growth is limited by the unknown timing of Quaternary overdeepening formation – meaning ice geometry during formation is also unknown – and by co-evolution of the ice surface slope as a result of reduced basal drag in overdeepenings due to till deposition and high basal water pressure.

Consideration of adverse slope gradient alone avoids the complexities introduced by co-evolution of the ice surface gradient. Adverse slope gradient values also demonstrate strong preferred peaks (Fig. 8I), and relationships between measures of overdeepening size and adverse slope gradient (e.g. Fig. 12A&B) imply a slowing of the rate of growth of overdeepening depth once a critical size threshold is reached, most notably for widths larger than

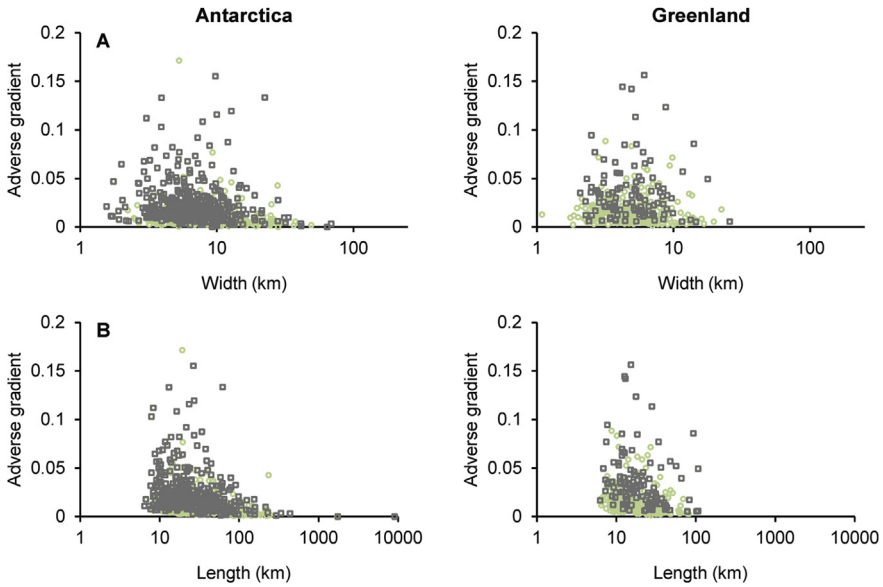

Fig. 12. Scatterplots of adverse slope gradient versus width and length.

10 km. In other words, gradients are steepest for median-sized overdeepenings, and the largest overdeepenings exhibit gradients that are lower than the preferred peak. This again supports a slowing of the rate of growth of overdeepening depth as a result of negative feedbacks, but implies that these are influenced not only by adverse slope gradient but also overdeepening size. Two reasons are plausible. First, insights into the development of equilibrium U-shaped valley forms obtained by Harbor (1992) indicate that the rate of widening of the overdeepening may decrease as it begins to impinge on the steeper sides of the U-shaped valley profile, where erosion potential is lower. Maintenance of the U-shape would then slow erosion at the overdeepening base but not prevent continued erosion at the overdeepening head and lip, thus permitting lengthening of the overdeepening and diminution of the adverse slope (Fig. 13A). In this scenario, the slightly larger size of overdeepenings in Antarctica might reflect the larger size of glacial catchments and larger valley widths. Second, increasing overdeepening size may cause a slowing of growth of overdeepening depth because a growing volume of sediment must be transported along the adverse slope (Fig. 13B&C), meaning the sediment that must be transported may overwhelm the capacity of available mechanisms. Evacuation of sediment from the floor of overdeepenings, which is necessary for further deepening, is then only likely to occur during episodes of glacier retreat when steep ice-surface gradients and strong melt promote steep hydraulic gradients.

4.2.4. Formation and evolution model

Cook and Swift (2012) concluded that mass-balance feedbacks and the limitations imposed by adverse slopes on subglacial water flow should cause glacier beds to grade toward a uniformly overdeepened long-profile (which might be termed an 'equilibrium' bed profile) that is dictated by the balance between the sediment transporting capacity by available mechanisms and the sediment supplied by erosion locally and upglacier. Whether such a balanced condition exists in nature is unknown, although large basins beneath the West Antarctic Ice Sheet that extend deeply into the ice sheet interior (cf. Joughin and Alley, 2011) may approach this condition to an extent. Elsewhere, it is likely that the complexity of processes involved in overdeepening initiation and evolution mean that bed morphology is typically highly complex.

The results of our study imply that this complexity can be explained by the stages of evolution shown in a simple conceptual model (Fig. 14). In this model, positive erosion feedbacks related to bed steepness, such as increased rates of abrasion motivated by faster sliding (e.g. Herman et al., 2011) and increased rates of quarrying motivated by both faster sliding and (where available) surface melt delivery (i.e. Hooke, 1991), initiate the growth of multiple overdeepenings in glacier beds. Positive feedbacks acting at overdeepening heads and negative ones acting on adverse slopes mean individual overdeepenings erode headward and coalesce (Fig. 14). Something akin to a uniform graded profile (cf. Cook and Swift) (Fig. 14F) may evolve in very mature and deeply eroded landscapes where there has been sufficient time for intervening bedrock highs (i.e. riegels) – if originally present – to have become denuded sufficiently for child overdeepenings to have fully coalesced.

This model explains our frequent observations of overdeepening nesting, and the tendency for individual child basins and parent basins to be asymmetric, with the deepest point occurring towards the overdeepening head. This pattern is likely to be most applicable to major outlet glacier systems. In the ice sheet interior, erosion potential is likely to decline because of slower basal sliding rates and the reduced volume of subglacial (and, in Greenland, surface) water. A further appealing aspect of our model is that it potentially accounts for shallower observed adverse slope gradients in Antarctica because Antarctic conditions – notably the absence of subglacially routed surface melt – imply lower capacities of sediment transport pathways and slower process rates at the bed.

4.3. Timing and timescales of overdeepening evolution

Similarity of 'preferred values' for overdeepenings in Greenland and Antarctica, despite the differing time periods of glaciation of their landscapes, indicates that overdeepenings reach such 'characteristic' dimensions within a maximum timeframe of ~2–3 million years (the period of glaciation in Greenland and also the time period for which regions of now cold-based ice in Antarctica are assumed to have undergone initial, warm-based glaciation; e.g. Bo et al., 2009). As such, the results indicate a minimum erosion

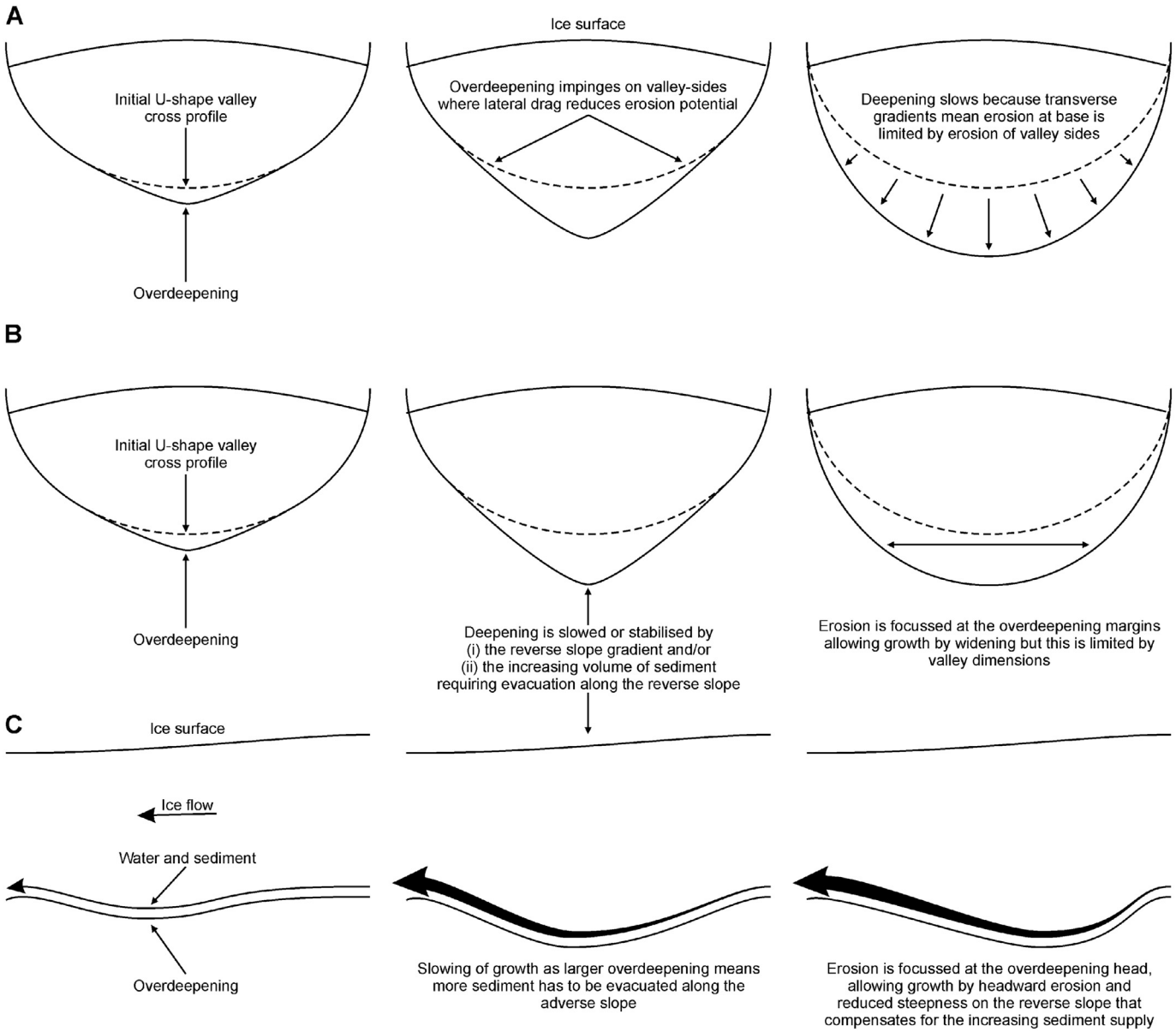

Fig. 13. Possible factors of influence on overdeepening depth and width that result in non-linear growth of depth, width and length. We do not assume that overdeepenings are necessarily U-shaped and assume that positive erosion feedbacks might initiate overdeepenings of non-U form. A. Slower ice flow near the valley margins causes the slowing of growth depth and width relative to overdeepening length. B and C: Growth of depth slows and depth ultimately stabilises because evacuation of sediment from the growing basin along the adverse slope exceeds the capacity of available sediment transport pathways, which causes sediment to be deposited within the basin. Width may continue to grow but this will be limited by valley width. Length continues to grow by headward erosion because freeze-on at the head entrains eroded material into the ice and hence headward growth is limited only by the catchment size. Headward growth of length may permit further deepening by reducing the adverse slope gradient, but the rate of deepening continues to slows due to the sediment evacuation constraints described above. Hence longer overdeepenings in the metric dataset have shallower adverse slope gradients than medium-sized overdeepenings (see text).

rate of 0.1 mm per year for a 200 m deep overdeepening, after which the rate of growth may in fact slow. This rate is entirely plausible, being an order of magnitude less than inferred rates of Quaternary ice sheet erosion of crystalline bedrock in Fennoscandia (e.g. Dowdeswell et al., 2010). However, this approach to erosion rate estimation has severe limitations, and a lack of age constraints means it is possible that even deep features may also have formed over similar (or even shorter) timescales if processes, or external controls such as lithology, allow far greater erosion rates in certain key locations. The heterogeneity of total subglacial erosion since the first glacial inception in Antarctica best reflects this, with modelled estimates ranging from 200 m in the ice-sheet interior to 2800 m within coastal troughs (Jamieson et al., 2010). Such divergent rates of erosion are consistent with field observations from present-day glaciers (Hallet et al., 1996).

The limited depth of overdeepenings in Antarctica and Greenland, which supports a 'slowing of growth' of overdeepening depth with age, contrasts with frequent observation of overdeepenings with depths >1000 m elsewhere in the Quaternary record. For example, overdeepenings of the Swiss Alpine foreland (Preusser et al., 2010) regularly exceed 1000 m in depth below local base level, and such depths are common for Norwegian fjords (e.g. Holtedahl, 1967). It is possible that subglacial bed topography datasets underestimate the depth of the deepest overdeepenings

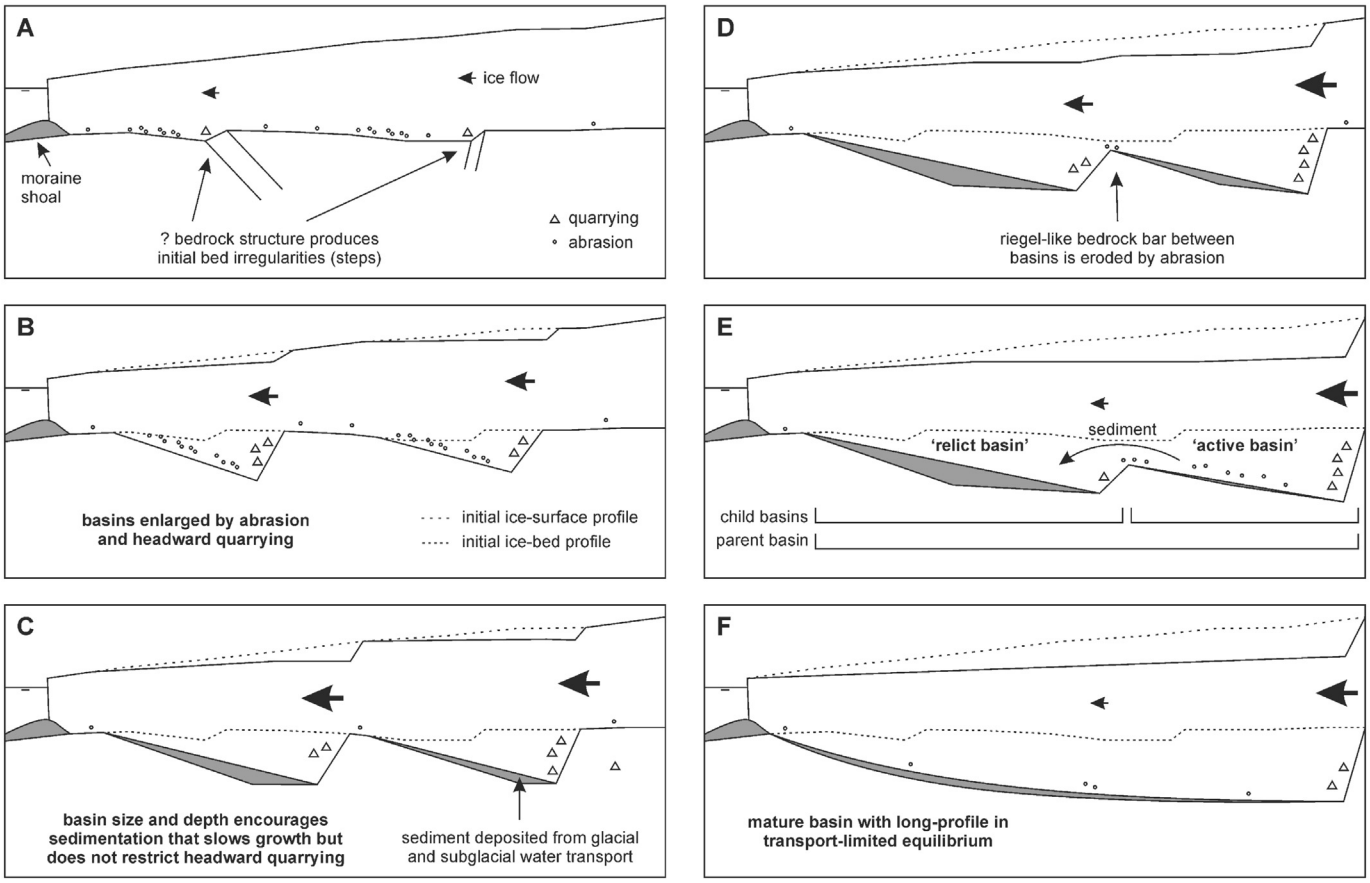

Fig. 14. A conceptual model of overdeepening evolution in ice sheet settings. The diagrams show the surface and bed of a topographically constrained outlet glacier along a ~100 km flow-parallel profile from the terminus. Initial bed irregularities (A) are amplified by bed-steepness (and, in Greenland, hydrological) feedbacks (B) that enhance sliding (arrows) and erosion at the overdeepening head; in addition, erosion at the head, particularly quarrying, produces debris that is used to abrade the adverse slope. As overdeepenings enlarge, sedimentation occurs on the adverse slopes (C), stabilising or slowing overdeepening depth, but permitting headward erosion. In addition, reduced subglacial drainage system transmissivity, leading to high basal water pressures and the deposition of a deformable sediment layer, reduce basal drag and cause a flattening of the ice surface above the overdeepening. Erosion becomes focused upon headwalls and the bedrock highs between overdeepenings (D) causing overdeepenings to merge, which may allow some evacuation of sediment from upglacier overdeepenings (E) that aids stabilisation of downglacier overdeepenings. The tendency will be for overdeepenings to be asymmetric and for upglacier overdeepenings to attain deeper profiles. Achievement of a uniform overdeepened-bed profile (F) (cf. Cook and Swift, 2012) occurs only in very mature settings.

because airborne radar surveys do not always resolve the ice-bed position where ice is particularly thick (Neil Ross, pers. comm.) or where subglacial lakes are present, but this cannot explain the strong preference for depths of ~200–300 m. Instead, it is possible that growth of overdeepening depth is more rapid in regions that are only occupied by ice during full glacial conditions, because repeated ice expansion and deglaciation is likely to lead to more frequent flushing of sediment from overdeepening floors. Notably, deglaciation is likely to lead to greater runoff from ice sheets, much of which will be routed via the bed, and a retreating ice margin will result in locally steeper ice surface gradients that drive steeper hydraulic gradients and, therefore, larger sediment transporting capacities. In contrast, in stable ice sheet settings, reduced drainage system transmissivity and sedimentation within overdeepenings is likely to reduce basal drag, leading to the flattening of the ice surface above and therefore a further reduction in the capacities of sediment transport pathways.

4.4. Limitations of datasets and metrics

The insights permitted by present datasets are subject to many limitations. Nonetheless, the sample sizes permitted by current data are sufficient for broad characteristics of overdeepening morphology and distribution to be discerned. Notably, distributions for many metrics demonstrate strong preferred values (e.g. Fig. 11) that are significantly larger than the minimum limits set by quality control criteria. This indicates that artefact depressions do not have a significant influence on the distribution shape. In addition, in many instances, the appearance of a preferred distribution peak is stronger for topographically confined depressions, for which a glacial origin is considered to be even more secure.

Another issue that our quality control criteria have tried to address is the long history of glaciation in Greenland and Antarctica, which raises the possibility that present landscape features were formed under ice sheet conditions that were substantially different. Notably, the cold-based regime of much of the Antarctic ice sheet since ~14 Ma has resulted in strong contrasts in the rates of glacial erosion (Jamieson et al., 2010; Thomson et al., 2013) that appear to have preserved many features from earlier in ice sheet history (Jamieson et al., 2014), and in Quaternary contexts such preservation appears to be common (e.g. Bierman et al., 2014; Davis et al., 2006; Goodfellow, 2007). For example, landscape features characteristic of temperate valley glaciation are preserved in the Gamburtsev Mountains, which are believed to have experienced erosive, warm-based conditions for only 2 million years (Bo et al., 2009; Rose et al., 2013). This issue is again addressed by the elongation criteria, which excludes features discordant with present ice flow. Further, most overdeepenings in

our dataset are associated with glacial valley and trough settings and therefore warm-based, fast-flowing, erosive ice (Cook and Swift, 2012) in which ice flow direction is likely to have been stable over many glacial cycles.

Finally, a challenge for future studies that aim to go further than we have done and relate overdeepening morphology to current ice sheet parameters is the extent to which processes that drive overdeepening formation operate sufficiently rapidly for overdeepening form to reflect current conditions imposed by today's ice sheet configuration. Erosion under warm-based ice conditions near the ice sheet margins has deepened many valleys by up to 2800 m, implying active erosion and sediment transport in these locations that should mitigate this problem. As a result, further confidence in the reliability of overdeepening metrics can again be achieved through focus on only those depressions where ice flow is topographically confined. Nonetheless, the timescales required for subglacial processes to adjust overdeepening morphology in response to changes in ice sheet forces are unknown. For Antarctica in particular, potentially slower rates of subglacial erosion and sediment transport may result in overdeepening morphologies remaining in disequilibrium. Given expectations that erosion and therefore landscape evolution is most rapid during early glacial cycles (cf. Koppes and Montgomery, 2009) at a time when the ice sheet was warmer, this implies that many features could reflect conditions that have prevailed early in ice sheet history.

5. Conclusion

Empirical data on overdeepening morphology and locations are much needed to advance understanding of ice sheet and landscape evolution processes. Knowledge of the processes that influence overdeepening depth and morphology is particularly needed because of its significance for (i) glacier and ice sheet stability, (ii) engineering applications, such as the long-term geological disposal of nuclear waste, and (iii) glacial and post-glacial evolution of topography (Cook and Swift, 2012). Data are also required to facilitate the testing of numerical ice-erosion models that permit investigation of ice-erosion feedbacks and instabilities that are produced by slow erosion processes occurring over thousands of years. Recent advances in such models justify the collection of high-quality data, including the increasingly sophisticated parameterisation of coupled transport and erosion processes (Egholm et al., 2012; Melanson et al., 2013) and the incorporation of higher order ice-sheet models capable of simulating ice flow at smaller length scales on steeper beds (Egholm et al., 2011; Pelletier et al., 2010).

Our mapping of topography beneath the present ice sheets confirms the ubiquity of overdeepenings in glaciated landscapes and provides new process insights. In addition, we highlight the potential advances that could be made using similar large datasets, notably because overdeepening location and morphology can be related directly to measurable ice sheet parameters, such as surface velocity (e.g. Patton et al., 2015). However, the limitations of present datasets necessitate strict quality control and limit the certainty of the insights that can be achieved.

Key observations from our dataset may be summarised as follows:

1. Overdeepenings beneath both ice sheets demonstrate strong morphological and dimensional similarities, although Antarctic overdeepenings tend toward larger values. The latter possibly reflects differences in the timescales of glaciation between the two continents, but potentially also the generally larger valley widths and catchment sizes of Antarctic outlet glaciers.
2. Overdeepening depth is skewed toward relatively low values of 200–300 m and median overdeepening depth in Greenland and Antarctica is very similar (around 170 m). Only a small proportion of overdeepenings beneath both ice sheets (around 8%) exceed 500 m depth.
3. Strong preferred values for width, length and depth indicate allometric growth of overdeepenings, although preference for relatively shallow depths and relationships between adverse slope gradient and overdeepening size indicate a ‘slowing of overdeepening growth’, particularly in terms of depth, with overdeepening size or maturity.
4. Topographic confinement exerts a significant additional control on overdeepening depth, with median depth values for confined overdeepenings being greater by 66 m and 123 m for overdeepenings in Antarctica and Greenland, respectively.
5. Overdeepening morphology is asymmetric, with the deepest point skewed toward the overdeepening head. In addition, the largest overdeepenings appear to have shallower adverse slopes, such that adverse slope is maximised for median-sized overdeepenings.
6. Overdeepenings are widespread beneath both ice sheets, and, in excluding many depressions where bed data resolution is low, our dataset represents a conservative estimate of the aerial extent of glacial overdeepening.

We interpret these observations to imply the following process-related conclusions:

1. Overdeepening asymmetry supports headward erosion, most likely as a result of quarrying, as the principal process of overdeepening initiation and evolution.
2. The observed ‘slowing of growth’ of overdeepening depth and the tendency for the largest overdeepenings to have shallower adverse slopes supports the existence of negative feedbacks related to hydrology and sediment transport that slow and stabilise overdeepening depth but do not necessarily restrict headward erosion and therefore overdeepening length.
3. In addition to the limitations placed by adverse slopes on subglacial water flow and their geomorphological implications, negative feedbacks that slow growth of depth may include the implications of increasing basin size for the volume of sediment that must be evacuated along the overdeepening adverse slope.
4. Preference for relatively shallow overdeepening depths and similarity of overdeepening depth for the two ice sheets despite their contrasting ice sheet histories further supports the proposed existence of stabilising feedbacks.
5. Slightly greater overdeepening depth and slightly steeper adverse slope gradients for topographically confined overdeepenings in Greenland versus those in Antarctica may arise from abundant surface melt, and possibly steeper ice surface gradients, that result in steeper subglacial hydraulic gradients that enhance sediment flushing.
6. Focussing of ice flow enhances erosion potential and overdeepening depth, but the presence of overdeepenings in diffluent settings (e.g. across continental shelf areas) and frequent nesting of overdeepenings supports the presence of positive feedback factors. For example, conditions that promote fast ice flow are likely to be responsible for overdeepenings that cross shelf areas that are far beyond the confining topography associated with their upstream outlet glacier systems.
7. The distribution of mapped depressions beneath large swathes of cold-based ice implies that many overdeepenings

are relict features, but a great many Antarctic overdeepenings are located in areas of deep glacial incision and fast ice flow, and this implies that erosion and sediment transfer rates in these locations may be comparable to those in Greenland. Elsewhere in Antarctica, the exact timing of overdeepening formation may be difficult to constrain, and recent, colder conditions may have further slowed subglacial erosion rates.

8. Evidence for a 'slowing of growth' means that 'mature' overdeepenings that are more useful for determining maximum limits to overdeepening depth are underrepresented in the dataset, and that erosion rates are difficult to infer using only morphological data. We speculate that the deepest overdeepenings are likely to form in locations where frequent climatic oscillations causing repeated glaciation allows locally steep hydraulic gradients during deglacial periods to fully evacuate sediment from deepening basins.
9. The wide variety of contexts of overdeepening formation, including diffluent settings, indicates possibly different origins. Unfortunately, those in shelf areas identified in this study constitute a sample that is too small to permit statistical investigation. Further work is required to solve the far from trivial problem of classifying overdeepening landscape context, from which differences in overdeepening origin and evolution may yet be found.
10. The presence of overdeepenings beneath fast flowing outlet glaciers and ice streams supports the idea that glaciological feedbacks associated with reverse bed slopes influence the flow mechanics and behaviour of these systems (cf. Cook and Swift, 2012).

We recommend that future studies undertake further investigation of overdeepening morphology in relation to ice sheet mass balance gradient and modelled ice sheet history (e.g. Golledge et al., 2013) as this is likely to provide more robust estimates of the time and conditions necessary to excavate overdeepenings of given size.

Acknowledgements

DAS thanks the National Cooperative for the Disposal of Radioactive Waste (Nagra), Switzerland, for their role in stimulating new research on the topic of focused glacial erosion, and DAS and HP further thank Nagra for funding the quantitative study of overdeepening morphology on which this paper is based (grant 11'716 Fcu/bys). HP also acknowledges support by the Research Council of Norway through its Centres of Excellence funding scheme (grant 223259) and the PetroMaks project "Glaciations in the Barents Sea area (GlaciBar)" (grant 200672). J.L. Bamber is thanked for access to the Greenland bed elevation dataset and F. Pattyn for providing modelled data relating to Antarctic basal thermal regime. Discussions with Andrew Sole and Jeremy Ely helped to advance ideas included in this study and we also acknowledge the valuable contribution made by participants of the overdeepening workshop held at the University of Sheffield in September 2013. Reviews by Roger Hooke and Stewart Jamieson resulted in substantial improvement to the manuscript and the quality of the dataset.

Appendix A. Supplementary data

Supplementary data related to this article can be found at http://dx.doi.org/10.1016/j.quascirev.2016.07.012.

References

Alley, R.B., Cuffey, K.M., Evenson, E.B., Strasser, J.C., Lawson, D.E., Larson, G.J., 1997. How glaciers entrain and transport basal sediment: physical constraints. Quat. Sci. Rev. 16 (9), 1017–1038.

Alley, R.B., Lawson, D.E., Evenson, E.B., Strasser, J.C., Larson, G.J., 1998. Glaciohydraulic supercooling: a freeze-on mechanism to create stratified, debris-rich basal ice: II. Theory. J. Glaciol. 44, 563–569.

Alley, R.B., Lawson, D.E., Larson, G.J., Evenson, E.B., Baker, G.S., 2003. Stabilizing feedbacks in glacier-bed erosion. Nature 424, 758–760. http://dx.doi.org/10.1038/nature01839.

Anderson, R.S., Molnar, P., Kessler, M.A., 2006. Features of glacial valley profiles simply explained. J. Geophys. Res. 111 (F1), F01004.

Augustinus, P.C., 1992a. Outlet glacier trough size-drainage area relationships, Fiordland, New Zealand. Geomorphology 4 (5), 347–361. http://dx.doi.org/10.1016/0169-555X(92)90028-M.

Augustinus, P.C., 1992b. The influence of rock mass strength on glacial valley cross-profile morphometry: a case study from the Southern Alps, New Zealand. Earth Surf. Process. Landforms 17 (1), 39–51. http://dx.doi.org/10.1002/esp.3290170104.

Bamber, J.L., Griggs, J.A., Hurkmans, R.T.W.L., Dowdeswell, J.A., Gogineni, S.P., Howat, I., Mouginot, J., Paden, J., Palmer, S., Rignot, E., Steinhage, D., 2013. A new bed elevation dataset for Greenland. Cryosphere 7 (2), 499–510. http://dx.doi.org/10.5194/tc-7-499-2013.

Batchelor, C.L., Dowdeswell, J.A., 2014. The physiography of High Arctic cross-shelf troughs. Quat. Sci. Rev. 92, 68–96. http://dx.doi.org/10.1016/j.quascirev.2013.05.025.

Bierman, P.R., Corbett, L.B., Graly, J.A., Neumann, T.A., Lini, A., Crosby, B.T., Rood, D.H., 2014. Preservation of a preglacial landscape under the center of the Greenland Ice Sheet. Science 344 (6182), 402–405. http://dx.doi.org/10.1126/science.1249047.

Bo, S., Siegert, M.J., Mudd, S.M., Sugden, D., Fujita, S., Xiangbin, C., Yunyun, J., Xueyuan, T., Yuansheng, L., 2009. The Gamburtsev mountains and the origin and early evolution of the Antarctic Ice Sheet. Nature 459 (7247), 690–693. http://dx.doi.org/10.1038/nature08024.

Clark, C.D., Hughes, A.L.C., Greenwood, S.L., Spagnolo, M., Ng, F.S.L., 2009. Size and shape characteristics of drumlins, derived from a large sample, and associated scaling laws. Quat. Sci. Rev. 28 (7–8), 677–692. http://dx.doi.org/10.1016/j.quascirev.2008.08.035.

Cook, S.J., Swift, D.A., 2012. Subglacial basins: their origin and importance in glacial systems and landscapes. Earth Sci. Rev. 115 (4), 332–372 [online] Available from: http://www.sciencedirect.com/science/article/pii/S0012825212001286 (accessed 23.10.13.).

Creyts, T.T., Clarke, G.K.C., 2010. Hydraulics of subglacial supercooling: theory and simulations for clear water flows. J. Geophys. Res. 115 (F3), F03021. http://dx.doi.org/10.1029/2009JF001417.

Davis, P.T., Briner, J.P., Coulthard, R.D., Finkel, R.W., Miller, G.H., 2006. Preservation of Arctic landscapes overridden by cold-based ice sheets. Quat. Res. 65 (1), 156–163. http://dx.doi.org/10.1016/j.yqres.2005.08.019.

Dowdeswell, J.A., Ottesen, D., Rise, L., 2010. Rates of sediment delivery from the Fennoscandian Ice Sheet through an ice age. Geology 35 (4), 359–362.

Egholm, D.L., Knudsen, M.F., Clark, C.D., Lesemann, J.E., 2011. Modeling the flow of glaciers in steep terrains: the integrated second-order shallow ice approximation (iSOSIA). J. Geophys. Res. 116 (F2), F02012. http://dx.doi.org/10.1029/2010JF001900.

Egholm, D.L., Pedersen, V.K., Knudsen, M.F., Larsen, N.K., 2012. Coupling the flow of ice, water, and sediment in a glacial landscape evolution model. Geomorphology 141–142, 47–66. http://dx.doi.org/10.1016/j.geomorph.2011.12.019.

Fretwell, P., Pritchard, H.D., Vaughan, D.G., Bamber, J.L., Barrand, N.E., Bell, R., Bianchi, C., Bingham, R.G., Blankenship, D.D., Casassa, G., Catania, G., Callens, D., Conway, H., Cook, A.J., Corr, H.F.J., Damaske, D., Damm, V., Ferraccioli, F., Forsberg, R., Fujita, S., Gim, Y., Gogineni, P., Griggs, J.A., Hindmarsh, R.C.A., Holmlund, P., Holt, J.W., Jacobel, R.W., Jenkins, A., Jokat, W., Jordan, T., King, E.C., Kohler, J., Krabill, W., Riger-Kusk, M., Langley, K.A., Leitchenkov, G., Leuschen, C., Luyendyk, B.P., Matsuoka, K., Mouginot, J., Nitsche, F.O., Nogi, Y., Nost, O.A., Popov, S.V., Rignot, E., Rippin, D.M., Rivera, A., Roberts, J., Ross, N., Siegert, M.J., Smith, A.M., Steinhage, D., Studinger, M., Sun, B., Tinto, B.K., Welch, B.C., Wilson, D., Young, D.A., Xiangbin, C., Zirizzotti, A., 2013. Bedmap2: improved ice bed, surface and thickness datasets for Antarctica. Cryosphere 7 (1), 375–393. http://dx.doi.org/10.5194/tc-7-375-2013.

Glasser, N.F., Crawford, K.R., Hambrey, M.J., Bennett, M.R., Huddart, D., 1998. Lithological and structural controls on the surface wear characteristics of glaciated metamorphic bedrock surfaces: Ossian Sarsfjellet, Svalbard. J. Geol. 106 (3), 319–330. http://dx.doi.org/10.1086/516025.

Glasser, N.F., Ghiglione, M.C., 2009. Structural, tectonic and glaciological controls on the evolution of fjord landscapes. Geomorphology 105 (3–4), 291–302. http://dx.doi.org/10.1016/j.geomorph.2008.10.007.

Golledge, Nicholas R., Levy, Richard H., McKay, Robert M., Fogwill, Christopher J., White, Duanne A., Graham, Alastair G.C., Smith, James A., Hillenbrand, Claus-Dieter, Licht, Kathy J., Denton, George H., Ackert Jr., Robert P., Maas, Sanne M., Hall, Brenda L., 15 October 2013. Glaciology and geological signature of the last glacial maximum Antarctic ice sheet. Quat. Sci. Rev. ISSN: 0277-3791 78, 225–247. http://dx.doi.org/10.1016/j.quascirev.2013.08.011.

Goodfellow, B.W., 2007. Relict non-glacial surfaces in formerly glaciated landscapes. Earth Sci. Rev. 80 (1–2), 47–73. http://dx.doi.org/10.1016/j.earscirev.2006.08.002.

Haeberli, et al., 2016. On the morphological characteristics of overdeepenings in high-mountain glacier beds. Earth Surf. Process. Landforms. http://dx.doi.org/

10.1002/esp.3966. Accepted Article.
Hallet, B., Hunter, L., Bogen, J., 1996. Rates of erosion and sediment evacuation by glaciers: a review of field data and their implications. Glob. Planet. Change 12 (1–4), 213–235. http://dx.doi.org/10.1016/0921-8181(95)00021-6.
Harbor, J.M., 1992. Numerical modeling of the development of U-shaped valleys by glacial erosion. Geol. Soc. Am. Bull. 104 (10), 1364–1375. http://dx.doi.org/10.1130/0016-7606(1992)104.
Harrowfield, M., Holdgate, G.R., Wilson, C.J.L., McLoughlin, S., 2005. Tectonic significance of the Lambert graben, east Antarctica: reconstructing the Gondwanan rift. Geology 33 (3), 197. http://dx.doi.org/10.1130/G21081.1.
Haynes, V.M., 1972. The relationship between the drainage areas and sizes of outlet troughs of the Sukkertoppen Ice Cap, West Greenland. Geogr. Ann. Ser. A Phys. Geogr. 54 (2), 66–75. http://dx.doi.org/10.2307/520543.
Herman, F., Beaud, F., Champagnac, J.D., Lemieux, J.M., Sternai, P., 2011. Glacial hydrology and erosion patterns: a mechanism for carving glacial valleys. Earth Planet. Sci. Lett. 310 (3–4), 498–508.
Holtedahl, H., 1967. Notes on the formation of fjords and fjord-valleys. Geogr. Ann. Ser. A Phys. Geogr. 49 (2/4), 188–203.
Hooke, R.L., 1991. Positive feedbacks associated with erosion of glacial cirques and overdeepenings. Geol. Soc. Am. Bull. 103, 1104–1108.
Jakobsson, M., Mayer, L., Coakley, B., Dowdeswell, J.A., Forbes, S., Fridman, B., Hodnesdal, H., Noormets, R., Pedersen, R., Rebesco, M., Schenke, H.W., Zarayskaya, Y., Accettella, D., Armstrong, A., Anderson, R.M., Bienhoff, P., Camerlenghi, A., Church, I., Edwards, M., Gardner, J.V., Hall, J.K., Hell, B., Hestvik, O., Kristoffersen, Y., Marcussen, C., Mohammad, R., Mosher, D., Nghiem, S.V., Pedrosa, M.T., Travaglini, P.G., Weatherall, P., 2012. The International Bathymetric Chart of the Arctic Ocean (IBCAO) Version 3.0. Geophys. Res. Lett. 39, L12609. http://dx.doi.org/10.1029/2012GL052219.
Jamieson, S.S.R., Sugden, D.E., 2008. Landscape evolution of Antarctica. In: Cooper, A.K., Barrett, P.J., Stagg, H., Storey, B., Stump, E., Wise, W., 10th ISAES Editorial Team (Eds.), Antarctica: a Keystone in a Changing World. The National Academic Press, USA, pp. 39–54.
Jamieson, S.S.R., Sugden, D.E., Hulton, N.R.J., 2010. The evolution of the subglacial landscape of Antarctica. Earth Planet. Sci. Lett. 293 (1–2), 1–27. http://dx.doi.org/10.1016/j.epsl.2010.02.012.
Jamieson, S.S.R., Stokes, C.R., Ross, N., Rippin, D.M., Bingham, R.G., Wilson, D.S., Margold, M., Bentley, M.J., 2014. The glacial geomorphology of the Antarctic ice-sheet bed. Antarct. Sci. 26 (6), 724–741. http://dx.doi.org/10.1017/S0954102014000212.
Jamieson, S.S.R., Vieli, A., Livingstone, S.J., Cofaigh, C.Ó., Stokes, C., Hillenbrand, C.-D., Dowdeswell, J.A., 2012. Ice-stream stability on a reverse bed slope. Nat. Geosci. 5 (11), 799–802. http://dx.doi.org/10.1038/ngeo1600.
Joughin, I., Alley, R.B., 2011. Stability of the West Antarctic ice sheet in a warming world. Nat. Geosci. 4, 506–513.
Joughin, I.B., Smith, B., Howat, I., Scambos, T.A., 2010. MEaSUREs Greenland Ice Sheet Velocity Map from InSAR Data. National Snow and Ice Data Center, Boulder, Colorado USA doi:nsidc-0478.001.
Jordan, T.A., Ferraccioli, F., Ross, N., Corr, H.F.J., Leat, P.T., Bingham, R.G., Rippin, D.M., le Brocq, A., Siegert, M.J., 2013. Inland extent of the Weddell Sea Rift imaged by new aerogeophysical data. Tectonophysics 585, 137–160. http://dx.doi.org/10.1016/j.tecto.2012.09.010.
Kessler, M.A., Anderson, R.S., Briner, J.P., 2008. Fjord insertion into continental margins driven by topographic steering of ice. Nat. Geosci. 1 (6), 365–369. http://dx.doi.org/10.1038/ngeo201.
Koppes, M.N., Montgomery, D.R., 2009. The relative efficacy of fluvial and glacial erosion over modern to orogenic timescales. Nat. Geosci. 2 (9), 644–647. http://dx.doi.org/10.1038/ngeo616.
Le Brocq, A.M., Hubbard, A., Bentley, M.J., Bamber, J.L., 2008. Subglacial topography inferred from ice surface terrain analysis reveals a large un-surveyed basin below sea level in East Antarctica. Geophys. Res. Lett. 35 (16), L16503. http://dx.doi.org/10.1029/2008GL034728.
Linton, D.L., 1963. The forms of glacial erosion. Trans. Pap. Inst. Br. Geogr. 33, 1–28.
Livingstone, S.J., Ó Cofaigh, C., Stokes, C.R., Hillenbrand, C.-D., Vieli, A., Jamieson, S.S.R., 2012. Antarctic palaeo-ice streams. Earth Sci. Rev. 111, 90–128. http://dx.doi.org/10.1016/j.earscirev.2011.10.003.
Lloyd, C.T., 2015. Controls upon the Location and Size of Glacial Overdeepenings. University of Sheffield, 1 March. [online] Available from: http://etheses.whiterose.ac.uk/8846/1/Christopher. Lloyd Thesis march2015.pdf (Accessed 26.11.15.).
Lundin, E.R., Doré, A.G., 2005. NE Atlantic break-up: a re-examination of the Iceland mantle plume model and the Atlantic – Arctic linkage. In: Dorè, A.G., Vining, B.A. (Eds.), Petroleum Geology: North-west Europe and Global Perspectives. The Geological Society, London, pp. 730–754.
Mazo, V.L., 1989. Waves on glacier beds. J. Glaciol. 35 (120), 179–182.
Melanson, A., Bell, T., Tarasov, L., 2013. Numerical modelling of subglacial erosion and sediment transport and its application to the North American ice sheets over the Last Glacial cycle. Quat. Sci. Rev. 68, 154–174. http://dx.doi.org/10.1016/j.quascirev.2013.02.017.
Morlighem, M., Rignot, E., Mouginot, J., Seroussi, H., Larour, E., 2014. Deeply incised submarine glacial valleys beneath the Greenland ice sheet. Nat. Geosci. 7 (6), 418–422. http://dx.doi.org/10.1038/ngeo2167.
Nick, F.M., Vieli, A., Howat, I.M., Joughin, I., 2009. Large-scale changes in Greenland outlet glacier dynamics triggered at the terminus. Nat. Geosci. 2 (2), 110–114. http://dx.doi.org/10.1038/ngeo394.
Patton, H., Swift, D.A., Clark, C.D., Livingstone, S.J., Cook, S.J., Hubbard, A., 2015. Automated mapping of glacial overdeepenings beneath contemporary ice sheets: approaches and potential applications. Geomorphology 232, 209–223. http://dx.doi.org/10.1016/j.geomorph.2015.01.003.
Pattyn, F., 2010. Antarctic subglacial conditions inferred from a hybrid ice sheet/ice stream model. Earth Planet. Sci. Lett. 295 (3–4), 451–461. http://dx.doi.org/10.1016/j.epsl.2010.04.025.
Pelletier, J.D., Comeau, D., Kargel, J., 2010. Controls of glacial valley spacing on earth and mars. Geomorphology 116 (1–2), 189–201. http://dx.doi.org/10.1016/j.geomorph.2009.10.018.
Preusser, F., Reitner, J.M., Schlüchter, C., 2010. Distribution, geometry, age and origin of overdeepened valleys and basins in the Alps and their foreland. Swiss J. Geosci. 103 (3), 407–426. http://dx.doi.org/10.1007/s00015-010-0044-y.
Rignot, E., Mouginot, J., Scheuchl, B., 2011. MEaSUREs InSAR-based Antarctica Ice Velocity Map. National Snow and Ice Data Center, Boulder, Colorado USA doi:nsidc-0484.001.
Rignot, E., Fenty, I., Xu, Y., Cai, C., Kemp, C., 2015. Undercutting of marine-terminating glaciers in West Greenland. Geophys. Res. Lett. 42 (14), n/a–n/a. http://dx.doi.org/10.1002/2015GL064236.
Rose, K.C., Ferraccioli, F., Jamieson, S.S.R., Bell, R.E., Corr, H., Creyts, T.T., Braaten, D., Jordan, T.A., Fretwell, P.T., Damaske, D., 2013. Early East Antarctic Ice Sheet growth recorded in the landscape of the Gamburtsev Subglacial Mountains. Earth Planet. Sci. Lett. 375, 1–12. http://dx.doi.org/10.1016/j.epsl.2013.03.053.
Röthlisberger, H., 1972. Water pressure in intra- and subglacial channels. J. Glaciol. 62, 177–203.
Schoof, C., 2005. The effect of cavitation on glacier sliding. Proc. R. Soc. A Math. Phys. Eng. Sci. 461 (2055), 609–627. http://dx.doi.org/10.1098/rspa.2004.1350.
Schoof, C., 2007. Ice sheet grounding line dynamics: steady states, stability, and hysteresis. J. Geophys. Res. 112, F03S28. http://dx.doi.org/10.1029/2006JF000664.
Shreve, R.L., 1972. Movement of water in glaciers. J. Glaciol. 11, 205–214.
Strachan, R.A., 1994. Evidence in north-east Greenland for late Silurian-early Devonian regional extension during the Caledonian orogeny. Geology 22 (10), 913–916. http://dx.doi.org/10.1130/0091-7613(1994)022.
Stump, E., Gootee, B., Talarico, F., 2006. Tectonic model for development of the Byrd glacier discontinuity and surrounding regions of the transantarctic mountains during the neoproterozoic — Early Paleozoic. In: Fütterer, D.K., Damaske, D., Kleinschmidt, G., Miller, H., Tessensohn, F. (Eds.), Antarctica - Contributions to Global Earth Sciences. Springer, Berlin, pp. 181–190.
Swift, D.A., Persano, C., Stuart, F.M., Gallagher, K., Whitham, A., 2008. A reassessment of the role of ice sheet glaciation in the long-term evolution of the East Greenland fjord region. Geomorphology 97 (1–2), 109–125. http://dx.doi.org/10.1016/j.geomorph.2007.02.048.
Thomas, R.H., 1979. The dynamics of marine ice sheets. J. Glaciol. 24, 167–177.
Thomson, S.N., Reiners, P.W., Hemming, S.R., Gehrels, G.E., 2013. The contribution of glacial erosion to shaping the hidden landscape of East Antarctica. Nat. Geosci. 6 (3), 203–207. http://dx.doi.org/10.1038/ngeo1722.
Timmermann, R., Le Brocq, A., Deen, T., Domack, E., Dutrieux, P., Galton-Fenzi, B., Hellmer, H., Humbert, A., Jansen, D., Jenkins, A., Lambrecht, A., Makinson, K., Niederjasper, F., Nitsche, F., Nøst, O.A., Smedsrud, L.H., Smith, W.H.F., 2010. A consistent data set of Antarctic ice sheet topography, cavity geometry, and global bathymetry. Earth Syst. Sci. Data 2 (2), 261–273. http://dx.doi.org/10.5194/essd-2-261-2010.
Weertman, J., 1974. Stability of the junction of an ice sheet and ice shelf. J. Glaciol. 13, 3–11.
Werder, M.A., 2016. The hydrology of subglacial overdeepenings: a new supercooling threshold formula. Geophys. Res. Lett. 43, 2045–2052. http://dx.doi.org/10.1002/2015GL067542.
Young, D.A., Wright, A.P., Roberts, J.L., Warner, R.C., Young, N.W., Greenbaum, J.S., Schroeder, D.M., Holt, J.W., Sugden, D.E., Blankenship, D.D., van Ommen, T.D., Siegert, M.J., 2011. A dynamic early East Antarctic Ice Sheet suggested by ice-covered fjord landscapes. Nature 474 (7349), 72–75. http://dx.doi.org/10.1038/nature10114.
Zwally, H.J., Abdalati, W., Herring, T., Larson, K., Saba, J., Steffen, K., 2002. Surface melt-induced acceleration of Greenland ice-sheet flow. Science 297 (5579), 218–222. http://dx.doi.org/10.1126/science.1072708.